Project report 2022

Scientific project design in drug discovery

Development of a Tetracycline for the prevention of heart failure with preserved ejection fraction following myocardial infarction

Professor:
Auwerx Johan

Supervisors:
Boulougouri Maria
El Alam Gaby
von Alvensleben Giacomo

Authors:
Castiglione Thomas, Hunter Agatha, Jemmi Emilie Letang - Mathieu Prunelle, Maille Coline, Marcandalli Elodie, Penfrat Emma, Pittet Gloria, Trifoni Francesca, Wettstein Maximilian

École Polytechnique Fédérale de Lausanne

Table of contents

Abstract

Heart failure (HF) affects more than 64 million people worldwide and is characterized by a high 5-year mortality rate, a poor quality of life, and high costs, resulting in a concerning global burden on the health care system. This qualifies heart failure as a global pandemic with half of all cases classified in heart failure with preserved ejection fraction (HFpEF). Improving care and treatment of HFpEF is thus a major public health priority since the prevalence of HFpEF continues to rise globally, likely because of the increasing number of patients affected by common risk factors such as hypertension and obesity. It is therefore not surprising that HFpEF is expected to be the prime HF contributor in the next years.

Cardiomyocytes, characterized by high energy consumption, are tightly dependent on correct mitochondrial functioning. Evidence shows that the accumulation of ROS is significantly enhanced in the failing myocardium, resulting in mitochondrial damage and reduced ATP production, eventually leading to cardiac remodeling, inflammation, and diastolic dysfunction in HFpEF. Fragmented mitochondria, cristae destruction, and a decreased mitochondrial area have also been described in HFpEF. Therefore, targeting mitochondrial dysfunction is an important therapeutic strategy for cardioprotection.

One critical pathway in mitochondrial homeostasis is the mitochondrial unfolded protein response (UPR^{mt}). Enhancement of the UPR^{mt} has been shown to yield important protective effects on cardiomyocytes such as increased ATP production, inhibition of oxidative stress injury, or inhibition of the release of apoptotic factors, therefore ameliorating mitochondrial and contractile dysfunction. These findings suggest that UPR^{mt} plays a key role in the stressed heart. UPR^{mt} can be activated by various means, one of them being electron transport chain (ETC) perturbations. There is evidence that disrupting mitochondrial ribosomes induces UPR^{mt} by generating a stoichiometric imbalance between nuclear and mitochondrial DNA-encoded respiratory chain subunits, thus leading to a perturbation in the ETC.

As shown in several studies, tetracyclines target mitochondrial ribosomes because of their similarities with their bacterial counterparts and, most importantly, that they can activate the UPR^{mt}. Furthermore, in addition to disrupting mitoribosomes, tetracyclines have many non-antimicrobial properties that qualify this class of compounds as a good candidate for the development of heart failure therapies such as ROS scavenging and inhibition of metalloproteases and inflammation.

In this report, we detail the preclinical and clinical development of a novel tetracycline drug targeting mitoribosomes to prevent HFpEF in hypertensive patients following myocardial infarction by inducing the mitochondrial unfolded protein response in cardiomyocytes.

1. Introduction

Heart failure (HF) is a global pandemic, affecting more than 64 million people worldwide[1]. Characterized by a 5-year mortality rate between 50% to 75%[1], poor quality of life, and high costs, HF is a concerning burden on healthcare expenditures. Of all cases, 50% correspond to heart failure with preserved ejection fraction (HFpEF)[2] and almost 5% of the population aged older than 60 has HFpEF[3]. Therefore, improving care and treatment of HFpEF is a major global public health priority, since HFpEF is expected to be the major HF player in the next years[1]. We propose to develop a novel tetracycline drug to prevent HFpEF in hypertensive patients following myocardial infarction by inducing the mitochondrial unfolded protein response in cardiomyocytes.

1.1 Heart failure with preserved ejection fraction (HFpEF) and existing treatments

Heart failure is defined as a "clinical syndrome with symptoms and/or signs caused by a structural and/or functional cardiac abnormality and corroborated by elevated natriuretic peptide levels and/or objective evidence of pulmonary or systemic congestion"[4]. The most common cause of HF worldwide is myocardial infarction (MI)[5], which induces cardiomyocyte death and scar formation, eventually leading to ventricular remodeling. Studies have shown that 41% of the patients rehospitalized for heart failure following acute myocardial infarction had heart failure with preserved ejection fraction (HFpEF)[6]. Heart failure with preserved ejection fraction, also known as diastolic heart failure, is characterized by normal left ventricular systolic function and abnormal diastolic function with left ventricular stiffness and hypertrophy, thicker and less elongated cardiomyocytes, higher collagen content, increased levels of natriuretic peptides, and an impaired relaxation after pumping blood out of the heart. The consequences of such features include decreased ventricular filling, higher diastolic pressure, and reduced lung compliance and cardiac output, leading to symptoms such as fatigue, weakness, dyspnea, orthopnea, paroxysmal nocturnal dyspnea, and edema[7].

Diagnosing HFpEF is often a clinical challenge, especially for patients at an early stage of the disease without clear signs of HF. Patients have to fulfill at least the three following criteria to be diagnosed with HFpEF: signs and/or symptoms of heart failure (such as shortness of breath, fatigue, irregular heartbeat, and more), no impaired systolic LV function (LV ejection fraction > 50 % and indexed LV end-diastolic volume < 97 ml/m²) and evidence of LV diastolic dysfunction[8]. Current diagnostic approaches mainly rely on echocardiography of normal ejection fraction and impaired diastolic function as well as natriuretic peptides measurement with suspected HF[9].

To this date, no treatments are available to fully cure the disease and the clinical treatments are mainly meant to ease the symptoms. Unlike heart failure with reduced ejection fraction (HFrEF), no medication classes to date have reduced cardiovascular or all-cause mortality in HFpEF[10]. This is attributed to the fact that HFpEF is a heterogeneous disease that involves multiple cardiac and extracardiac pathophysiological abnormalities[11]. However, most clinical trials have targeted all patients with HFpEF and led to varying responses to treatment[12].

Most common forms of HFpEF have been associated with metabolic diseases, such as diabetes mellitus, present in half of the HFpEF patients, or morbid obesity in more than 60% of HFpEF cases[13]. Moreover, hypertension predicts HFpEF in 75% of the cases[14]. HFpEF comorbidities have been shown to trigger a systemic pro-inflammatory state which leads to coronary microvascular endothelial inflammation and dysfunction[15]. This state increases the production of reactive oxygen species (ROS) which favors hypertrophy and increased stiffness of cardiomyocytes and contributes to diastolic dysfunction and heart failure development. Usually, it is a fatty acid oxidation increase that increases the production of ROS. However, depending on the comorbidity, fatty acid oxidation either increases (diabetes and obesity) or decreases (hypertension)[16]. Whether specific treatment of these subgroups improves the outcome of HFpEF treatment has yet to be determined. Therefore, the classification of HFpEF patients and the development of targeted therapies could offer major benefits[14].

1.2 Mitochondrial unfolded protein response (UPR^{mt}) as a cardioprotective target

Mitochondria serve as cellular powerhouses responsible for ATP production, with reactive oxygen species (ROS) being generated as byproducts that are rapidly neutralized by cellular antioxidant mechanisms in normal conditions. Cardiomyocytes, characterized by high energy consumption, are tightly dependent on correct mitochondrial functioning and ROS play an important role in regulating their growth and death[17]. It has been shown that accumulation of ROS is significantly enhanced in the failing myocardium, resulting in mitochondrial damage and reduced ATP production, eventually leading to cardiac remodeling, inflammation, and diastolic dysfunction in HFpEF[18] The mitochondrial metabolism in HFpEF is characterized by increased fatty acid uptake and decreased glucose oxidation, associated with decreased oxidative phosphorylation[3]. Furthermore, fragmented mitochondria, cristae destruction, and a decreased mitochondrial area have been described in HFpEF[3]. Therefore, targeting mitochondrial dysfunction is an important therapeutic strategy for cardioprotection.

A critical pathway in mitochondrial homeostasis is for example the mitochondrial unfolded protein response (UPR^{mt}), activated when misfolded proteins accumulate within mitochondria and lead to increased expression of mitochondrial chaperones and proteases to maintain protein quality and mitochondrial function. Enhancement of the UPR^{mt} has been shown to ameliorate mitochondrial and contractile dysfunction, suggesting an important protective role in the stressed heart[19]. The protective effects of the UPR^{mt} on cardiomyocytes under stress include increased ATP production, inhibition of oxidative stress injury induced by excessive accumulation of ROS, inhibition of the release of apoptotic factors, inhibition of calcium overload, and inhibition of the abnormal opening of the mitochondrial membrane permeability transition pores[20]. In fact, these findings suggest that the targeting of the UPR^{mt} has great potential as a therapeutic strategy for heart failure.

The UPR^{mt} can be activated by various means, one of them being electron transport chain (ETC) perturbations[21]. It has been shown that disrupting mitochondrial ribosomes induces UPR^{mt} by generating a stoichiometric imbalance between nuclear and mitochondrial DNA-encoded respiratory chain subunits, thus leading to a perturbation in the ETC[22] (Figure 1). The usage of tetracyclines to perturb mitochondrial function and induce a certain amount of stress could appear as paradoxal while it is generally accepted that this would cause harmful effects. However, these insults to the mitochondria induce an adaptative reparative response termed mitohormesis, where low levels of ROS are generated which in turn activate protective signaling pathways such as UPR^{mt}[23]. Therefore, we propose to develop a compound that impairs mitoribosome functioning to induce the UPR^{mt} in cardiomyocytes.

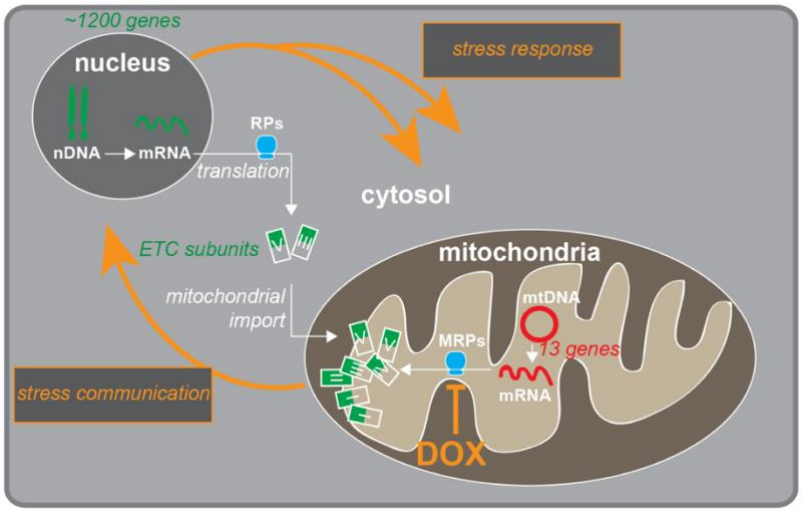

Figure 1. Disrupting mitochondrial ribosomes induces UPR^{mt} by generating a stoichiometric imbalance between nuclear and mitochondrial DNA encoded respiratory chain subunits[16].

1.3 Tetracyclines

Tetracyclines were first discovered in 1945 when chlortetracycline was isolated from the bacterium Streptomyces aureofaciens[24]. Since then, many other members of the tetracycline family have been developed and tetracyclines are nowadays one of the most widely used antibiotic compounds in clinical applications worldwide.

All members of the tetracycline family comprise of a backbone of four aromatic rings to which a variety of functional groups are attached[24]. The antimicrobial effect is achieved by targeting the bacterial ribosome, mainly by binding on a high-affinity site located on the 30S subunit, thus halting protein synthesis[24]. More specifically, the primary binding site of tetracyclines is located at the base of the small subunit, thus blocking the binding of aminoacyl-tRNA to the A-site.

Just like the mitochondria itself, mitoribosomes have evolved from bacterial ribosomes[25]. However, mitochondrial ribosomes have diverged from their bacterial ancestors, leading to differences in configuration and structure. While bacterial ribosomes are made from a 50S large subunit (LSU) and a 30S small subunit (SSU), mitoribosomes are made of a 39S LSU and 28S SSU. Still, tetracyclines can inhibit mitochondrial translation by targeting mitochondrial ribosomes because of their similarities with their bacterial counterparts[26]. Most importantly, tetracyclines have been shown to activate the UPR^{mt} in several studies[27,28].

In addition to their antibiotic effects, tetracyclines have many non-antimicrobial properties that qualify this class of compounds as a good candidate for the development of heart failure therapies. These characteristic features include ROS scavenging, inhibition of protein aggregates, metalloproteases, inflammation, and apoptosis which are all cardioprotective targets[26]. For our project, we thus focus on identifying new compounds in the tetracycline family able to inhibit mitoribosomes, resulting in the activation of the UPR^{mt} in cardiomyocytes.

1.4 Drug development process overview

The goal of this report is to detail the drug development process of a novel drug belonging to the tetracycline family to prevent HFpEF in hypertensive patients following myocardial infarction. We start with a virtual screening phase, with first a structural and then a ligand-based virtual screening, to identify potential hit candidates, followed by *in vitro* primary assays to reduce the number of selected compounds. Secondary toxicity assays as well as optimization of the structure and mechanisms are performed afterward to identify the compounds that meet important criteria that we defined. The molecules selected from the above-mentioned steps are first validated *in vivo* on mouse models then safety is assessed on healthy dogs (since the older diseased human heart may be dog-like[29]) before entering clinical trials to test the efficacy of our hit-to-lead choice. The latest is validated if several criteria are

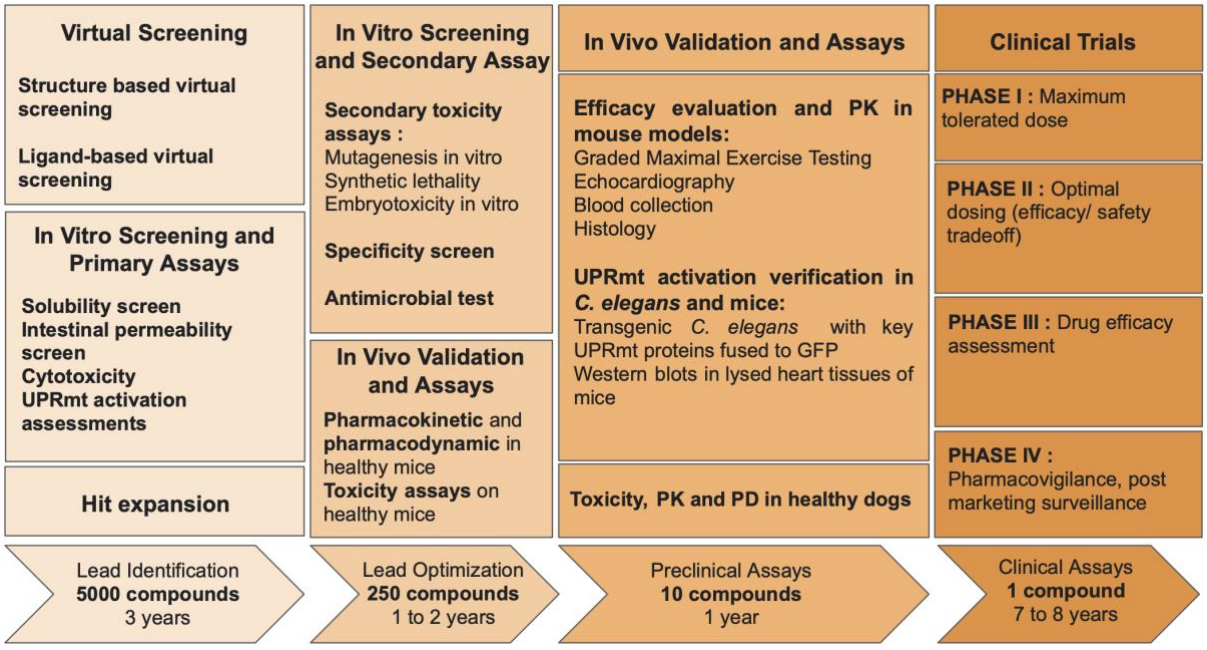

Figure 2. Flow chart summarizing the drug development process, consisting of the identification of lead compounds, lead optimization via in vitro and in vivo assays, preclinical assays on animal models, and clinical trials.

met, such as an increased exercise tolerance[30], a normal diastolic function or a decrease in specific biomarkers[11]. The detailed drug development process is described in the following flow chart (Figure 2).

2. Virtual screening

To generate a baseline library of 5000 candidate compounds for *in vitro* screening, virtual screening is first performed. The main objective is to prioritize drug candidates by reducing the compound chemical space that is explored with subsequent *in vitro* screening. Depending on the results, the affinity of the obtained library to our target is also partially optimized. This task is performed using the software LEA3D[31].

2.1 Virtual screening strategy using LEA3D

LEA3D offers two main screening strategies: *de novo small molecule design* and *virtual screening.* The first uses a modified Genetic Algorithm to modify a baseline ligand library across generations to maximize a docking score. At each generational step, it evaluates the fitness of all ligands by comparing docking scores, keeps the best ones, constructs a new library by modifying them (cross-over, mutations), and starts again until a termination criterion is met. This method is helpful when the goal is to design a ligand without strong conditions on its chemical structure. In the context of this project, this strategy is not well suited since we want our lead compounds to be part of the tetracycline family, meaning having the same structural, physical, and chemical properties, which would not necessarily be respected with *de novo small molecule design*. However, this strategy offers two options to condition the generated compounds on a given molecule. The first one is by adding a component to the scoring function reflecting how structurally close a generated molecule is to a reference molecule and maximizing it. The second one is to start the Genetic Algorithm from a base structure (in this case Tetracycline) and add chemical fragments at given atoms. Both options are assessed but they do not ensure the conservation of the tetracycline family properties.

The second strategy, *virtual screening*, is very well suited to the task since it screens a given library of compounds and scores them by their binding affinity. It can therefore be given a library of compounds belonging to the tetracycline family only. A library containing 741 molecules belonging to the tetracycline family is retrieved from PubChem[32] and used for *virtual screening.*

Both strategies calculate docking scores using the docking program PLANTS[33], which is based on a modified *ant colony optimization* algorithm to solve the protein-ligand docking problem. In short, PLANTS works by exploring the combinatorial space of the ligand-binding site complex and guides the exploration in directions that minimize the given objective function, which is based on interaction potentials. The scores given by LEA3D output are percentages derived from the ChemPLP PLANTS score, which models the van der Waals interactions and repulsion potentials[34].

The parameters used for LEA3D jobs are available in Supplementary Table 1.

2.2 Limitations of the selected strategy

The mitoribosome is a highly heterogeneous compound, containing 80 proteins and 3 large ribosomal RNA molecules[35]. A complete structure file of the whole mitoribosome is not available at the time of this study. However, there is no need for such a structure since we are only interested in the tetracycline primary binding site on the 30S SSU sub-domain, as explained in section 1.3. A structure file of the 30S SSU sub-domain is retrieved from Kaushal et al.[36] Still, the selected cryo-EM structure of the whole mammalian mitoribosome SSU presents some drawbacks for virtual screening.

First, the structure does not contain Mg^{2+} ions which are used by tetracyclines as binding cofactors[37]. However, the docking algorithm used by LEA3D does not consider solvent nor free ions interactions in its docking algorithm, so the presence of Mg^{2+} ions should not change the outcome of the docking, even though it should result in inaccurate docking modeling.

Secondly, as the entire structure file is too large for the used virtual screening software, a new structure is generated by introducing a cutoff radius of 75Å from the center of the primary binding site, i.e., only atoms that are closer than 75Å to the center of the binding site in the 3D structure file are retained. The choice of this threshold is made by visually checking that the whole binding pocket was contained. This whole preprocessing is performed using Pymol[38] and python.

Third, from the literature, Tetracycline binds to the S16 double-stranded RNA of the 30S subdomain. After discussion with a developer of LEA3D, it was concluded that LEA3D/PLANTS do not take RNA molecules into account, it removes them from the input PDB file. This strongly disrupts the whole experiment as tetracyclines bind to RNA only and the binding site contains almost no amino acids as shown in Figure 3.

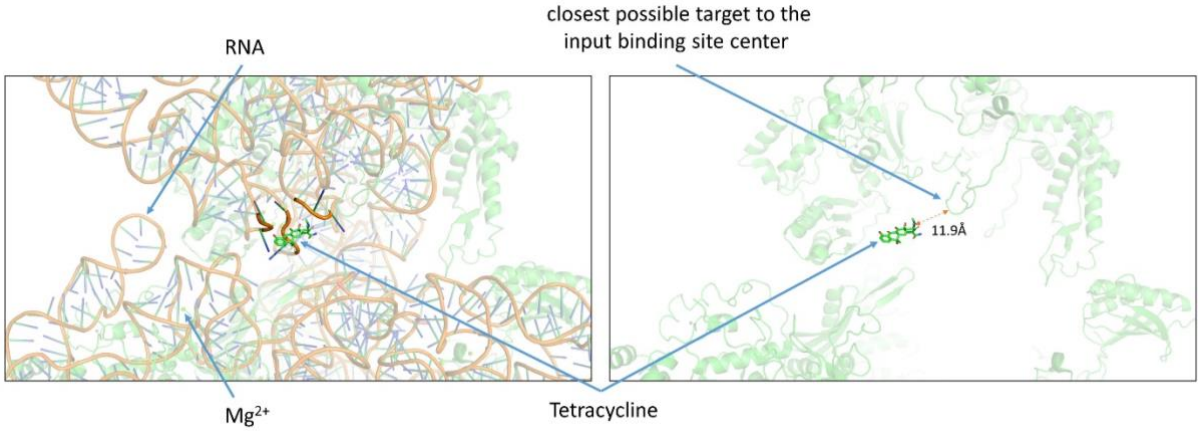

Figure 3. Tetracycline bound to the primary binding site on the mitoribosome S30 SSU sub-domain. **Left:** containing Magnesium ions and RNA molecules. The atoms closer than 3.5Å (maximum distance of H-bonds) to the Tetracycline molecule are highlighted. **Right:** without Magnesium ions and RNA molecules. The right image shows how the target is used by LEA3D, which visibly discards most of the binding site. The closest distance between the Tetracycline and the protein is 11.9Å.

2.3 Identified lead candidates

Due to the limitations mentioned above, especially LEA3D not taking RNA into account, all results obtained with this tool must be taken as informative only as the compounds are not docked to the target RNA molecule but to its protein surroundings.

2.3.1 *De novo* small molecules design

The top 3 compounds from the LEAD3D *de novo small drug design* starting from the Tetracycline molecules retrieved from PubChem (ID 54675776) are shown in Figure 4 below. The docking scores are very high (90% to 100%), a hypothesis for this behavior could be that the long oxygen branches (colored in red on the structures) form several hydrogen bonds with the protein loop they bind to as shown in Figure 3 (verified with Pymol).

3D structure	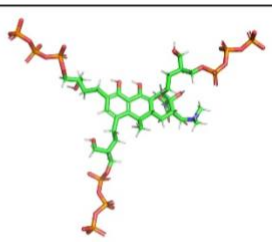	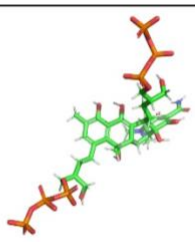	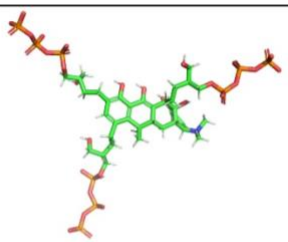
Score (%)	100.00	97.19	93.19

Figure 4. Top 3 compounds from *de novo* small molecule design starting from the Tetracycline molecule.

2.3.2 Tetracyclines library virtual screening

The top 3 compounds from the *virtual screening* library retrieved from PubChem are shown in Figure 5 below. The docking scores are relatively low, but this could be due to the limitations explained in section 2.3, mainly the loss of most of the binding site.

2D structure	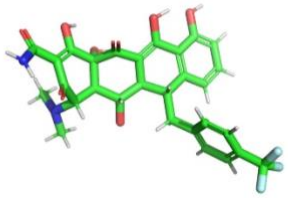	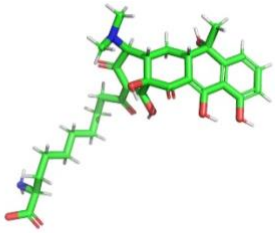	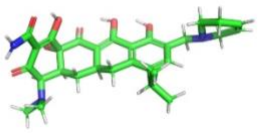
Score (%)	70.3	69.99	68.92
PubChem ID	69471110	160035247	126545662

Figure 5. Top 3 compounds from virtual screening of the tetracycline family library.

2.4 Improvement proposal

To address LEA3D constraints, we further improve the results by using other virtual screening softwares. Existing frameworks taking RNA from the target compound into account are accessible such as DOCK[39] and ICM[40].

After having selected a base lead compound library from successful virtual screening simulations, other *in-silico* analyses are performed to further characterize, refine, and reduce the selected library. This is done by analyzing criterions such as ADMET (absorption, distribution, metabolism, excretion, and toxicity), solubility, and Ames mutagenicity predictions using ADMET Predictor®[41]. Binding kinetics predictions (using ProBound[42]) and synthetic accessibility estimations are performed using metrics defined in Ertl P. *et al.*[43]. The library of lead compounds can then be expanded by adding chemical groups to key positions in each compound, considering the Synthetic Accessibility of these modifications. Finally, the selected lead candidate library is synthesized and used for the *in vitro* screening phase.

3. *In vitro* screening

The virtual screening is followed by *in vitro* primary and secondary assays which seek to evaluate the physical properties, efficacy, pharmacodynamics, and toxicity of the previously selected compounds to reduce their amount. During the primary assays, the aim is to select 250 candidates to enter the secondary assays whose best compounds can move forward to the *in vivo* validation phase.

3.1 Primary assays

The candidates selected during the virtual screening are first screened for solubility, intestinal permeability, and cytotoxicity to evaluate their pharmacodynamics in the body as well as their potential toxic side effects. Their interaction with our chosen target is then evaluated using FRET, and NMR spectroscopy. The activation of the UPR^{mt} pathway is be verified in human immortalized cardiac cell lines.

3.1.1 Solubility screen

Solubility is an important parameter in drug development, as the active molecule must go through specific environments with varying temperatures and pH levels. This physicochemical parameter needs to be identified early in drug development; specifically, it is important to verify the solubility for absorption after oral administration[44].

The ideal solubility of a drug is a value bigger than 60 µg/mL. An equilibrium solubility assay can be performed by mixing an excess of the drug with a buffer for a few days until saturation. The sample that is obtained is then filtered and can be quantified using High-performance liquid chromatography (HPLC).

Kinetic solubility assays offer a high throughput method by using a small amount of compound and a shorter incubation time. For this purpose, a small volume of a concentrated stock solution (usually DMSO) is added to the buffer. The solubility can then be determined by nephelometric assay where undissolved particles are detected with a light scattering, the sample can then be filtered, and the dissolved material can then be quantified using UV absorption[45].

3.1.2 Intestinal permeability screen

The Caco-2 screening assay is frequently used *in vitro* to determine intestinal permeability and drug efflux. It is a standard method for orally administered drugs to evaluate the passive and active transport and absorption of the drug in the intestine. Caco-2 cells have characteristics that resemble the intestinal epithelium and are composed of a polarized monolayer, intracellular junctions, and a brush border on the apical side[46]. By measuring the flux rate of the compound across the cells, we can approximate its intestinal permeability. Using this method, we can determine the transport in both directions, from the apical side to the basolateral side and vice-versa of the Caco-2 cells which indicates the active efflux of the compound in the intestine[47].

The experiment consists of introducing the compound on either the apical or basolateral side of the monolayer. After a certain amount of time, the buffer on each side of the Caco-2 monolayer is removed and the different concentrations of the compound are calculated using liquid chromatography-mass spectrometry (LC-MS) and LC-tandem mass spectrometry (LC-MS-MS). This experiment is repeated for different lengths of time[48].

3.1.3 Cytotoxicity screen

The main aim of the cytotoxicity screens is to assess whether the target compounds have long or short-term toxic effects on the body, for example by inhibiting key cell functions such as ATP production. We perform several assays which are mainly based on fluorometric, and fluorescent measurements of markers associated with cell viability, cell proliferation, or cell damage in HeLa cell lines.

The first assay we perform is a Tetrazolium-based assay such as an MTT test. These tests are based on the principle that the mitochondria of viable cells can reduce MTT into purple-colored Formazan by harnessing the reducing power of NADH. The change of color can then be measured by fluorometry. A luciferase-based assay is then executed to measure ATP production in cells which acts as a marker of viable cells. This assay is based on the catalytic property of luciferase which emits light when it reacts with ATP yielding a fluorometric readout. These two first assays have the benefit of being very easy to perform and can therefore be done in high throughput as well as being readily available in ready-to-use kits. However, as only cell viability can be assessed, we perform additional assays to examine the effects on cell proliferation.

One key mechanism that can be assessed during cell proliferation is DNA synthesis. To do so, BrdU, a thymidine analog that is progressively incorporated into DNA upon replication, can be added to the cells. Its presence can then be measured using BrdU-specific antibodies. As this assay is based on antibodies, it requires prior DNA degradation which can degrade the sample. Therefore, another thymidine analog, EdU, can be used instead or in conjunction with BrdU. This analog has the advantage of being able to be fused to a fluorophore and allows a quantitative readout without requiring DNA degradation.

In addition to those assays, matrix metalloproteinases (MMPs) are other proteins whose expression is to be checked during a tetracycline treatment. Indeed, it has been shown that there is a decrease in matrix degradation in hypertensive patients with HFpEF, due to the downregulation of MMPs. This can lead to an increased collagen synthesis which facilitates myocardial fibrosis. However, tetracyclines are also known to inhibit those MMPs. It is therefore necessary to test for the toxicity of tetracyclines regarding their impact on MMPs.

3.1.4 Fluorescence Resonance Energy Transfer (FRET)

After assessing the solubility, intestinal permeability, and cytotoxicity of the initial library of compounds, we test the interaction with the target using Fluorescence Resonance Energy Transfer or FRET, to further reduce the pool of molecules selected in the previous section. FRET is one of the most dominant methods for high-throughput screens. It can determine protein-protein interaction very precisely and has a high sensitivity. Its process consists of labeling the molecules of interest, here the 28S SSU sub-domain of mitoribosomes and the tetracyclines compounds with fluorescent molecules. The drug candidates are excited with light and usually labeled with Yellow Fluorescent Protein whereas mitoribosomes are not excited and are labeled with Cyan Fluorescent Protein[49]. When binding occurs, i.e., the distance between the 2 compounds is very low (<10nm), the excited fluorescent molecule on the drug emits energy and transfers it to the fluorescent molecule of the bound mitoribosome, which becomes excited and emits energy[50]. This method has several advantages. It can be very flexible due to its large spectrum of wavelength and choice of fluorescent molecules. The user of this method can choose the fluorescent molecules of their interest, with the constraint that the excitation spectra of the fluorescent molecule that emits energy overlaps with the absorption spectra of the fluorescent molecule that accepts energy. Moreover, this method is distance sensitive and does not have any off-target effects as a signal is emitted only if binding occurs. It is also one of the cheapest methods to test protein-protein interactions as it does not require specific instruments, as flow cytometry protein interaction assay and NMR spectroscopy do. However, FRET measurements can have a low signal-to noise ratio, which can make the analysis difficult, and can be impacted by the environment of the experiment since fluorescent proteins are sensible to changes in temperature and pH[51]. Therefore, a second assay assessing the mitoribosomes-tetracyclines interactions is important to confirm the results and increase their accuracy.

3.1.5 NMR spectroscopy

To further assess the candidate tetracycline-mitoribosome interactions, Nuclear Magnetic Resonance (NMR) spectroscopy is performed. There are currently two kinds of NMR spectroscopy methods: target-resonance and ligand-resonance-based methods. The NMR-

based assay is performed with methods based on ligand-resonance, as they do not require isotope labeling contrary to target-resonance methods, are faster and usually requires a smaller quantity of drug to work. Target Immobilized NMR Screening (TINS) is selected here as it seems to work efficiently independently of the size and chemical composition of the target[52]. As the mitoribosomes are much bigger in size than the usually targeted proteins, the TINS method is indeed a useful method to obtain reliable results. The TINS method can also determine high-affinity binding drugs. In this process, the targeted molecule, here mitoribosomes, are immobilized on a support such as streptavidin Sepharose in NMR tubes. A control tube containing only the support is added as a reference for the 1D H1 NMR spectral analysis. Once the drug is administered, the tubes containing the mitoribosomes and the control samples are passed through the spectrometer and their NMR spectra are subtracted to obtain the NMR spectra of the mitoribosomes-drug interactions[53]. Competitors of tetracyclines can also be added to test their effect on their interaction with the mitoribosomes.

3.1.6 UPR^{mt} activation verification in Human cell lines

As the aim of our drug is to activate the UPR^{mt} pathway to induce cardioprotective properties, it is essential to screen for its activation by our target compounds. As a first step, this is done on human cell lines and, later, in *C. elegans* and mice to validate the results for our candidate drugs (cf. section 4.4).

We aim to verify the drug candidates for UPR^{mt} activation in AC16 human cardiomyocyte cell lines, as they have the same mitochondrial function as cardiomyocytes[54]. This allows us to better predict the effect of the screened drugs in patients. To test for the pathway activation, we harness the fact that in UPR^{mt} there is an imbalance between the mitochondrially and nuclear encoded parts of the oxidative phosphorylation pathway, a phenomenon termed mitonuclear discordance[22,55]. We therefore perform a Western blot against MTCO1, a mitochondrial encoded gene, and ATP5A, a nuclear encoded protein, and measure the ratio between the two genes, as they are representative of nuclear and mitochondrial gene expression in the oxidative phosphorylation pathway. An overexpression of the nuclear encoded gene compared to the mitochondrially encoded gene allows to show UPR^{mt} activation in these cell lines.

The assay enables us to determine with confidence whether the drug candidate(s) activate the UPRmt pathway, and those that successfully do so are selected for the next round of screening.

3.2 Secondary assays

Following primary *in vitro* assays, the top 250 drug candidates are further subjected to secondary assays to evaluate more precisely their properties and potential toxicity for human cells as well as for bacteria and to assess their ability to activate the UPR^{mt} pathway in cardiomyocytes.

3.2.1 Secondary toxicity assays

The first test in the secondary toxicity assays is the mutagenesis screening. We perform this test in order to know which of our drug compounds can lead to genetic mutations and rejecting them for our final drug. To do this experiment, the cells are exposed to compounds that may cause DNA damage. If this damage is not repaired, it causes mutations. To prevent this, the cells have developed DNA repair methods to lower the accumulation rate of genetic mutations over time[56]. Multiple test combinations assess the effects of the three major endpoints of the genetic damage associated with human diseases:[57] gene mutation (point mutations or deletions/insertions), clastogenicity (structural chromosome changes) and aneuploidy (numerical chromosome aberrations).

The Ames test allows the drug to cause changes in the DNA and detect the point mutations, deletions, and insertions. We select different strains of *Salmonella* which carry different mutations in multiple genes in the histidine operon. The strains are cultured on agar plates containing minimal histidine and only the strains that revert to histidine independence

can grow. If the strains grow, we can determine which of our tetracyclines compounds induces mutations, and based on this, mutagenic drug candidates are eliminated[57].

To assess how a certain substance can potentially induce point mutations, clastogenicity and aneugenicity, we perform the *in vitro* micronucleus test. This test is done by using either mammalian cell lines or primary human cell cultures such as cardiomyocytes, lymphocytes, or fibroblasts. Micronuclei (MNi) are expressed in dividing cells that have chromosome breaks or whole chromosomes that are unable to migrate during mitosis. For the *in vitro* micronucleus test, the cells are cultured until chromosome damage leads to the formation of MNi, and then the MNi amount is scored. This score reflects the toxicity concentration dependence of the compound[58].

The next step is to test the combination of drugs with our compounds. Synthetic lethality is used to understand the mechanism of action of drugs[59]. This strategy requires drug combinations, when simultaneously administrated, to cause the cell's or even the organism's death. It is important to screen drugs for synthetic lethality since not all interactions are known or wanted. Besides, it is good to know interactions between molecules to combine therapies and predict the drug effects[60]. Therefore, in this test, we try multiple combinations of our tetracyclines compounds with common drugs. We selected 100 of the most used drugs for other heart diseases, 50 of the most used drugs for hypertension, and 50 of the most used drugs in general, giving a total of 200 drugs that our target population is susceptible to taking. The compounds are tested by exposing cardiomyocytes simultaneously to one of our drugs and another molecule of the selected drug list. Within a few hours of the drug's exposure, we score the cells' viability, if there are many dead cells, the combination of our compound with the other drug is synthetically lethal and we decide that the two drugs can't be taken together.

After verifying that our tetracycline compound is not dangerous for the subjects, we want to ensure that it has no repercussions on reproduction. Embryotoxicity is any morphological or functional alteration caused by chemical or physical agents that interferes with normal growth, homeostasis, development, and differentiation of the fetus. This test allows assessing if our drug has toxic effects on reproduction. It is important as we don't want any repercussions on future lives.

The Embryonic Stem Cell Test (EST) is a good first test to do before animal model studies, it is reliable and validated scientifically *in vitro* system for testing embryotoxicity[61]. Here we use human embryonic stem cells. These endpoints are assessed to predict the embryotoxic potential of a substance[62]: the inhibition of differentiation into several different cell types such as cardiomyocytes, the cytotoxic effects on stem cells, cytotoxic effects on 3T3 fibroblasts and unknown differentiation patterns. The cells are exposed to our compounds, and the lethality and embryo malformation that results from the exposure is measured. Furthermore, the cells are exposed to the drug at different embryogenesis stages[62,63].

3.2.2 Specificity Screen

To assess the absence of off-target effects of our drug candidates, a specificity screen is further performed.

Off-target effects are investigated via a ligand binding assay (LBA). LBA relies on the binding of ligand molecules to receptors, antibodies, or other macromolecules. A detection method is used to determine the presence and extent of ligand-receptor complexes, and this is usually determined electrochemically or through a fluorescence detection method.

In our case, we expose our candidate drug to a panel of enzymes or proteins to investigate their off-target interactions. Those libraries are commercially available and among them, we choose to test in priority the activation of kinases[64], gapless, and of different receptors[65]. The results from those assays are tightly related to the toxicity assays discussed above, as they could allow us to better understand the off-target toxic effects caused by certain metabolites. LBA should also be performed in the *in vivo* validation assays, to assess the systemic effects and whole-tissue effects on the different animal models presented in section 4.

3.2.3 Antimicrobial test

To assess the antimicrobial effect of our candidate molecules, we perform antimicrobial susceptibility testing (AST) which aims to identify which antimicrobial regimen is specifically effective for individual patients[66].

Tetracyclines are a family of antibiotic molecules, and to determine the level of induced mitochondrial stress, we use an AST. Indeed, we aim to lower antimicrobial effects, thus triggering mitohormesis, designated as a biological response where the induction of a reduced amount of mitochondrial stress leads to an increment in health and viability within a cell, tissue, or organism. We aim to preserve the beneficial properties of tetracycline in the context of HF, such as ROS scavenging, inhibition of protein aggregates, metalloproteases, inflammation, and apoptosis, as mentioned in section 1.4. According to Bárcena and Al[67], the beneficial outcomes of mitohormesis are most probably due to an increase in mitochondrial ROS and the positive benefits exerted by mitohormesis are associated with UPR^{mt} activation. The increase in the production of ROS is a characteristic of HFpEF, as mentioned in section 1.1 and the UPR^{mt} activation pathway is targeted by our candidate drug.

A variety of methods can be used to evaluate or screen the *in vitro* antimicrobial activity of a compound via AST. We selected the disk-diffusion assay because of its high efficacy, low complexity, and low cost. This assay can also be used to test for antimicrobial susceptibility *in vivo*[67,68]. Another option would be to use agar dilution methods in case the results generated with the disk-diffusion assay are not satisfactory.

To perform the disk-diffusion method, first, a standardized inoculum from a bacterial culture needs to be prepared, suspended, and standardized using McFarland standards as the reference to adjust the turbidity of the bacterial suspension in a tube. This helps to ensure that the number of bacteria is within a given range to standardize microbial testing[69]. The next step is to inoculate the bacterial suspension to a particular growth medium (e.g., Mueller Hinton Agar, MHA for disk diffusion) and add the antimicrobial disks. The plates are then incubated. Finally, we can measure the zone of inhibition using a dedicated instrument and interpret the AST results.

4. *In vivo* validation

Once *in vitro* validation is completed, we proceed with the analysis of the selected compounds on healthy mice by profiling parameters such as pharmacokinetics, pharmacodynamics, and toxicity to screen for the 10 most promising ones. These are tested on mice models and healthy dogs to choose the final molecule. The *in vivo* validation is essential to achieve higher information about the therapeutic potential of the drug and the determination of the optimal oral dosage that should be given to the patients during their treatment.

4.1 Pharmacokinetic (PK) and pharmacodynamic (PD) profiling in healthy mice

Pharmacokinetic (PK) and pharmacodynamic (PD) are two determinant factors for establishing the effects of a drug candidate in an *in vivo* setting. To profile these parameters, and help in the optimization of the drug's dosage, we have to assess the following parameters: absorption, distribution, metabolism, and excretion (ADME). These four characteristics are determined for each of the selected compounds resulting from the *in vitro* assessments in healthy mice.

Given its efficiency, as the first level of in vivo screening, a Rapid Assessment of Compound Exposure (R.A.C.E) is performed. This screening method allows the determination of the relationship between the effects of a novel chemical probe and a measure of its concentration, representing its absorption and elimination pharmacokinetics attributes.

For the conception of this *in vivo* PK screening, several doses of compounds are formulated. At three of the four mice used for each experiment, a dose equivalent to 5-50 mg/kg is orally given, and the fourth is the vehicle. Thereafter, two-time points for blood collection are provided, the first at t = 20 min and the second at t = 120 min. The samples are then collected and analyzed through LC-MS/MS. The resulting data are used to construct the curve of the concentration of the compound in plasma (C_p) as a function of time. The area under the curve ($AUC_{t=20,\ t=120}$) of each test compound is then compared, this provides enough information to estimate a rank order of the compound exposure to the administered dose[70]. Test compounds with a larger $AUC_{t=20,\ t=120}$ are suitable for further screening, as they show better absorption into tissues and thus a greater chance of producing a biological effect.

To achieve greater efficiency and safety of the assays, compounds that show promising overall exposure are subjected to a second level of screening called Comprehensive Pharmacokinetics Analysis. For proper sampling, a minimum of six mice are required for each tested compound, and each of them receives a 2 mg/kg dose by oral gavage. Afterward, over the following 24 hours, 9 times points are planned to collect blood samples, precisely at t = 5, 15, 30 min, 1, 2, 4, 8, 24 hours. Blood samples collected are analyzed by LC-MS/MS. The results are reported as a response curve where the plasma drug concentration is plotted as a function of the elapsed time. PK parameters such as the area under the curve (AUC), the half-life ($t_{1/2}$), the maximal plasma concentration (C_{max}), time of maximal concentration (t_{max}) the clearance (CL) and the oral bioavailability, are obtained from the curve (see. Figure 6.)[70].

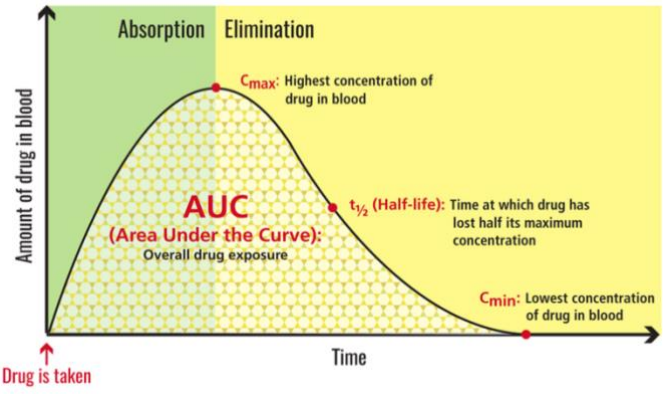

Figure 6. Pharmacokinetics and area under the curve (AUC). AUC is a measure of how much drug reaches a person's bloodstream in a given period of time after a dose is given.

Once the PK absorption profiles have been determined, the distribution of the remaining compounds within the tissues is studied. Several screenings are proposed to optimize the results. Only the organs of primary interest (those targeted by our drug and those most affected by mitochondrial dysfunction) are analyzed.

First, to analyze drug distribution, mice are sacrificed at C_{max}. Then the heart, the liver, and the brain, are analyzed by mass spectrometry. The latter is necessary to determine whether the drug has not crossed the blood-brain barrier (BBB). Afterward, the volume of distribution (V_D) is calculated to estimate the amount of drug necessary to reach a given plasma concentration. V_D is represented by the ratio of the drug dose present in the tissue of interest and its plasma concentration when the distribution of the drug is at equilibrium, reached when the entry and exit rates between blood and tissue are equivalent[71].

Subsequently, a pharmacodynamic approach, which involves the oral administration of different doses of drugs based on their PK characteristics, is carried out to test the action of the remaining compounds. Mice are sacrificed at regular timepoints until reaching T_{max} and then are perfused to remove the blood from tissues. In this way, we can be sure that the compound measured is the one that has been absorbed by the tissue of interest and not the one still presents in the blood. We finally perform an LC-MS/MS analysis to quantify the abundance of the compounds.

Prioritized compounds then undergo Quantitative whole-body autoradiography (QWBA). This method consists of placing a ^{14}C radioactive tag, with a radioactivity range between 1.5-100 µCi/kg[72], at a metabolic stable site of the candidate drug, followed by oral administration to mice. This *in vivo* experiment allows the visualization of the radio-labeled compound distribution and concentration within all tissues and organs, in addition to continuous tracking of the drug's circulation[73]. The different radioactivity levels are calculated through the exposure of a thin cross-section of the dosed animal to a phosphor-imaging screen, followed by a scan with a phosphor imager[72]. The working principle of a phosphor-imaging screen is based on a screen containing a thin layer of crystal that absorbs and stores energy emitted by the radioactive material[74].

During this study, which duration is determined by the half-life of our radiolabeled compound, for further evaluation of long-term safety, we also proceed with a mass balance study (MBS) to profile metabolic characteristics and excretion pathways. This consists of the collection of plasma, urine, and fecal samples at regular intervals every 2 hours throughout all the study periods. The radioactivity and the metabolite are analyzed and profiled at each step. A High-performance liquid chromatography (HPLC) screening is used for a qualitative and quantitative analysis leading to the determination of the metabolic profiles of plasma samples over time[72]. In the end, a complete profile of the total radioactivity in the plasma over time is obtained, which can be compared with a profile of the parent drug obtained by LS/MC/MC for validation[72].

Finally, to examine whether our drug has activated the UPR^{mt}, we aim to determine which genes are induced and which proteins are translated. For this purpose, we compare the heart biopsy of mice subjected to a candidate drug to control mice by sequencing the samples using RNAseq. Using the results of a differential expression analysis comparing treated samples to controls, gene set enrichment analysis is performed to identify significantly enriched molecular processes. RNAseq is complemented by proteome mapping to determine the effect of the candidate drug at the protein level. With those two *omic* layers, we provide a molecular profile for each tested molecule. This allows us to see whether important proteins characterizing UPR_{mt}, such as Activation Transcription Factor 5 (ATF5), Activation Transcription Factor 4 (ATF4), and C/EBP homologous protein (CHOP)[75] have been induced. This also allows us to determine which pathways have been affected and whether apoptotic genes have been activated.

4.2 Toxicity assays in healthy mice

An important part of developing a drug lies in identifying its main side effects. Preclinical studies are a crucial part of establishing these effects. To this end, PK and PD parameters are used to assess duration and dosage in toxicology assays for the evaluation of the safety, the efficacy, the limitations, as well as the possible off-target effects.

For this purpose, an *in vivo* micronucleus assay is performed in the bone marrow of young healthy mice, which should ensure active bone marrow division. For 10 days, mice are administered with three different dose levels determined by the parameters C_{max} and AUC achieved in the PK and PD studies. An initial limiting dose represents the maximally tolerated dose (MTD) before reaching lethality (MTD is often about 1000 mg/kg), followed by a mid-dose equivalent to half of the limiting dose and a low-dose, half of the mid-dose, which still should have visible pharmacodynamic effects. Two other groups of mice are included in the experiment: the vehicle, and the positive control. Vehicle mice are administered with a physiological saline solvent which doesn't produce a chemical reaction and control mice with cyclophosphamide, which is known to induce micronuclei[76]. The mice are then sacrificed, and the bone marrow is extracted from the femur. Cells are then stained, and enterocytes are counted and scored by light microscopy to gain additional information for micronuclei presence[77]. The existence of small additional nuclei in enterocytes is a direct indication of genotoxicity, which indicates the presence of genotoxic agents that could cause chromosomal aberrations related to serious health effects, such as immune dysfunction, cancer, or spontaneous abortions [78].

Subsequently, immunotoxicity is evaluated by assessing parameters such as changes in immunoglobulin levels, histopathological changes of the thymus and the spleen, and stress-related immune changes. If one of these toxicology assays shows an adverse immune effect, an additional immune function study assay, T-cell dependent antibody response (TDAR), is performed on potentially intoxicated mice. For this purpose, blood samples are collected during the study and suspended with sheep red blood cells (SRBC), which are used to recognize and bind to T-Cells. The high antibody response is then detected and quantified through an enzyme-linked immunosorbent assay (ELISA)[79].

With the candidate molecules passing the toxicology tests, toxicokinetic tests are performed to observe the systemic exposure to our compound and the relation with the administered dose within the duration of the study. We test at the three doses concentrations mentioned before. At several time points, blood samples are collected, and the concentration of our compound is measured. These results contribute to determining if our compound is safe[80].

Carcinogenicity studies are then performed by systemic exposure and by exceeding the maximum dosage. The length of this test usually corresponds to the targeted administration duration in patients, here at 24 weeks. During these 24 weeks, we give our drug to 10 healthy mice. At 12 and at 24 weeks we sacrifice 5 mice. We look if some of the mice have developed any tumors or abnormal masses near the heart zone. If this is not the case, the candidate drug is considered as not carcinogenic[80].

Reproductive toxicology assays are also performed to verify the absence of effects on reproduction. We perform two main tests: the Fertility and Early Embryonic Development (FEED) test and the Embryo-Fetal Development (EFD) test. For the FEED test, the drug treatment is administered before mating on both male and female mice to assess whether there are any consequences on the mating or the embryos. The aim of the EFD test is to observe the effects on pregnant female mice and how the drugs affect the embryo and fetus. If there are clear indications of malformations or lethality of the fetus, the candidate drug is not considered safe [81]. The dosage and exposure of the reproductive experiments are the same as the one projected for the clinical trials.

Finally, antibiotics often disrupt the gastrointestinal microbiome, which regulates many functions, justifying the evaluation of the candidate compounds' effects on the gut microbiome.

Moreover, as we previously did an antimicrobial test in vitro, we aim here to confirm the results in vivo. Fecal samples are collected before and after the administration of the drug. The microbial DNA of the samples are analyzed and compared with bacterial databases to determine the potential side effects of the tested compounds[82].

4.3 Efficacy and pharmacokinetics in HFpEF mouse models

To evaluate the efficacy and pharmacokinetics of our drug candidates on the pathophysiology of HFpEF, *in vivo* validation experiments are performed in two hypertensions induced HFpEF mouse models shown to mimic the human disease phenotype.

4.3.1 Mouse models recapitulating HFpEF

The first model proposed for the *in vivo* assays is the aldosterone-infused and unilateral nephrectomized mouse model. Studies have shown that the ablation of one kidney combined to the infusion of aldosterone and administration of 1% sodium chloride (NaCl) induces blood pressure elevation, cardiac hypertrophy, fibrosis and circulating aldosterone levels comparable to the ones seen in human acute heart failure (18ng/ml on average)[83]. If infused for 4 weeks following uninephrectomy, these mice develop HFpEF accompanied with moderate hypertension, concentric LV hypertrophy, pulmonary congestion, and diastolic dysfunction while maintaining a normal/preserved LVEF[84]. Exercise impairment increased cardiac size as well as increased natriuretic peptides, which are all features also observed in human HFpEF patients[41,85].

Aldosterone is the main mineralocorticoid steroid hormone produced by the adrenal glands. It is part of the renin-angiotensin-aldosterone system (RAAS) that regulates blood pressure, fluid and electrolyte balance, and systemic vascular resistance by increasing the effective circulating volume, extracellular fluid volume, and blood pressure. Aldosterone expression is induced by angiotensin II and binds to mineralocorticoid receptors in the distal tubules and collecting ducts of the nephron, leading to the reabsorption of sodium and excretion of potassium in the kidney, thereby indirectly influencing water retention, blood pressure, and blood volume[86]. Accordingly, increased levels of aldosterone result in hypertension and stimulation of collagen synthesis by myocardial fibroblasts, resulting in left ventricular hypertrophy with tissue fibrosis and myocardial stiffness. The aldosterone-infused uninephrectomized mouse model thus appears as a promising animal model to recapitulate the pathogenesis of HFpEF and study the effect of our drug candidate *in vivo*.

The angiotensin II-infused mouse model can be used as a second model to recapitulate HFpEF as it also induces cardiac hypertrophy and remodeling, diastolic dysfunction, preserved LVEF, as well as pulmonary congestion, and exercise intolerance after infusion for two to eight weeks[87]. However, cardiac hypertrophy appears to be strain-specific, as C57BL/6J mice develop concentric hypertrophy while Balb/c mice show severe LV chamber dilatation, which is not characteristic of HFpEF[88]. Furthermore, diastolic dysfunction and preservation of LVEF are likely dose-dependent[87]. The chosen strain and dosage should thus be optimized in the experimental design to obtain a relevant HFpEF model.

4.3.2 Experimental design and efficacy assessment

To evaluate the efficacy of our candidate drugs, tests are performed in three main mouse populations of a total of 20 mice each, both male and female in equal amounts: control healthy mice, aldosterone-infused uninephrectomized mice, and angiotensin II-infused mice. The C57BL/6J mouse strain is chosen for the three models because of the reasons explained above. Uninephrectomy is performed on day 0 of the experiment for the aldosterone-infused model. Mice are then infused with either aldosterone and 1% NaCl or angiotensin-II for 4 weeks to induce hypertensive HFpEF in both models.

It is important to emphasize that the mouse models proposed here do not involve the onset of a myocardial infarction prior to developing HFpEF. Since the goal is to initially test the

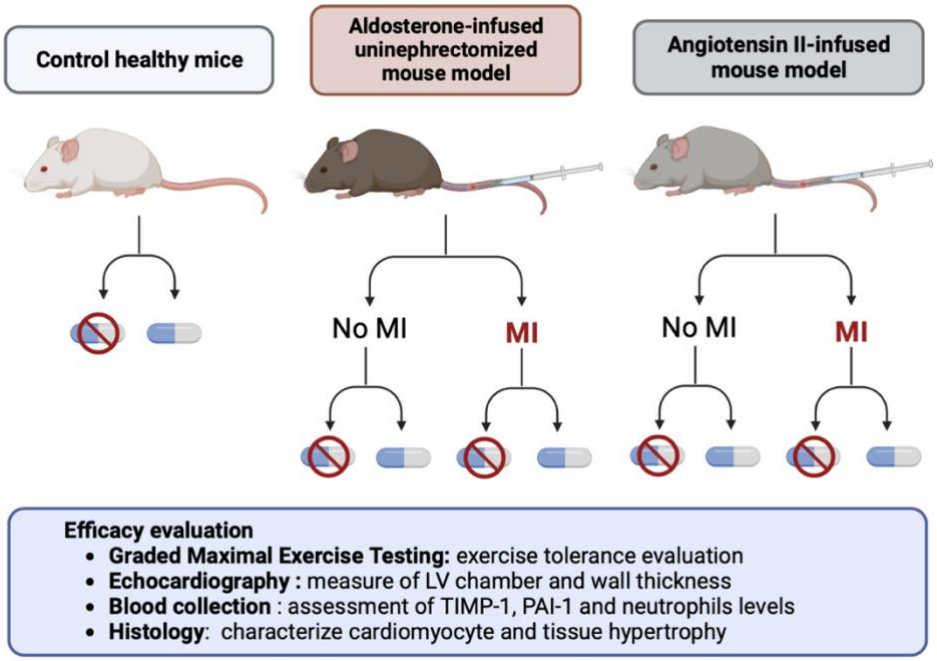

Figure 7. Experimental design for the *in vivo* validation tests of the candidate drugs. Two hypertension-induced HFpEF models are used along with control healthy mice. Mice are then separated into four different groups for each model: MI or no MI, and treatment or control. The efficacy of the drugs is then assessed with different tests. Created with *BioRender.com.*

capacity of the candidates in post-MI patients, our *in vivo* experiments should include a first step mimicking a MI in our mouse models, to recapitulate the pathogenesis of the targeted patient population. The mice in the two hypertension-induced HFpEF models are thus separated into two groups on day 14 post uninephrectomy and one group is surgically operated to ligate the left anterior descending artery, the most common way used to mimic myocardial infarction[89]. The two groups are then further separated into two different groups (treated vs non-treated) and simultaneously administered with either the drug candidates or solvent every day for 2 weeks, in addition to the already present aldosterone or angiotensin-II infusion The experimental design is illustrated in Figure 7.

From our knowledge, the induction of MI during aldosterone or angiotensin-II infusion has not been tested in mice, rising potential concerns about the feasibility of this experiment. However, findings suggest that mice tend to maintain sufficient cardiac function following large infarcts, thus allowing assessment of injury for several weeks following MI and suggesting that our experimental design could function properly[90]. Still, the dosage of the different compounds should be optimized to prevent the death of the mice prior to the end of the treatment. We include tests in normal hypertension-induced HFpEF mouse models (non-MI) to compare the effects of our candidates with MI mice and expand the assessment of the efficacy of our drugs in HFpEF patients without experiencing previously an MI.

Throughout the treatment, several parameters are tested to measure the efficacy of the compounds. First, cardiovascular fitness (CVF) is assessed weekly by graded maximal exercise testing (GXT), which has improved mouse-exercise testing sensitivity compared to speed progress until exhaustion (PXT), to evaluate exercise tolerance in all mice groups[91]. GXT is tested by measuring oxygen consumption (VO2) to obtain $VO2_{max}$ (the peak oxygen consumption when RER is >1), carbon dioxide expiration (VCO2), and run-time until exhaustion, defined as the point at which mice maintained continuous contact with the shock grid for 5 seconds, during treadmill running with concurrent staged increases in running speed and inclination. We expect to detect a difference in time until exhaustion, derived from VO2 kinetics between the treated and the untreated mice, with the last group reaching exhaustion faster.

Then, transthoracic echocardiography (TTE) specific to small animals is performed bi-weekly to evaluate the ventricular function of the mice. The evaluation of HFpEF in mouse models requires assessing the presence of preserved left ventricular ejection fraction (LVEF), a diastolic function indicator, and the development of HF which is allowed by TTE[92]. Indeed,

LVEF can be obtained by acquiring images in a short-axis view and by calculating the volume according to the Teichholz formula, and the presence of diastolic dysfunction in mice can be indicated by left atrial (LA) enlargement[49]. Mice that model the disease and didn't receive the treatment are expected to show HFpEF development, specifically with an LVEF and a LA enlargement, compared to the mice without the administration of our compounds.

Blood samples are collected every second day to measure the concentration of specific HFpEF biomarkers. Elevated natriuretic peptide levels, such as natriuretic peptide B-type (BNP) or N-terminal pro-brain natriuretic peptide (NT-proBNP), carry significant prognostic implications as those hormones are released in response to cardiomyocyte stretch[93]. Assessed in plasma or in LV tissue, increased levels of natriuretic peptides due to the presence of elevated LV filling pressure are observed in angiotensin II or aldosterone-infused mice model[94]. Therefore, treated mice are expected to experience reduced natriuretic peptide blood concentration compared to untreated ones. It also has been shown that, in hypertensive patients with HFpEF, there is a decrease in matrix degradation due to the downregulation of matrix metalloproteinases (MMPs) and upregulation of tissue inhibitors of matrix metalloproteinases (TIMPs)[2]. This leads to an increased collagen synthesis which facilitates myocardial fibrosis[95] (that's why we checked for tetracycline toxicity on MMPs on the section 3.4.3 of the report). When excess TIMP-1 is detected in blood samples, it may indicate HFpEF development in patients with hypertension. In a similar way, increased plasminogen activator inhibitor-1 (PAI-1) expression has been shown to be implicated in cellular aging, senescence, and most HFpEF comorbidities[11]. Indeed, PAI-1 is a key protein secreted by metabolically unhealthy visceral adipose tissue, which is found in the vast majority of HFpEF patients[96]. Therefore, treated mice are expected to have increased TIMP-1 and/or PAI-1 blood concentration, detected, and quantified by ELISA, with respect to the untreated mice. As those biomarkers levels are used in HFpEF prognostics in humans, TIMP-1, PAI-1, and natriuretic peptide are used as variables of efficacy in human clinical trials (see section 5.1).

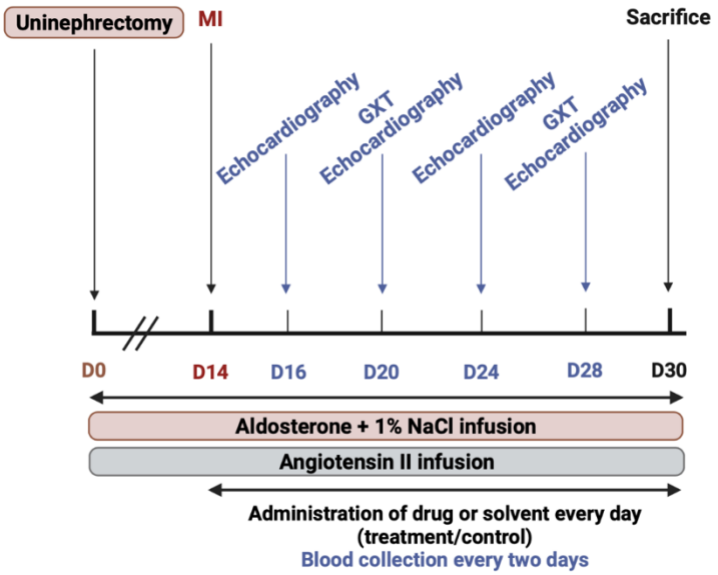

Figure 8. Experimental timeline of the *in vivo* validation experiments. Aldosterone-infused mice are uninephrectomized on day 0. Both models are then infused with either aldosterone and 1% NaCl or angiotensin-II for 4 weeks. On day 14, MI is induced in subgroups of both models and mice are administered for the remaining two weeks with either our candidates or solvent. Efficacy evaluation tests are performed during the last two weeks. Created with *BioRender.com.*

Finally, mice are sacrificed on day 30, and histology of the cardiac tissue is performed to characterize cardiomyocytes and assess tissue hypertrophy. Other tests, described in the following section, are performed in lysed heart tissues of mice to assess the activation of the UPR^{mt} pathway in cardiomyocytes. The whole experimental timeline is illustrated in Figure 8.

4.4 UPR^{mt} activation verification in *C. elegans* and mice

The aim of this section is to test if our target can activate the UPR^{mt} pathway in mice and *C. elegans* upon binding to the mitochondria. This, together with the tests done on human cell lines, can indicate whether our drug is able to activate this pathway in the heart of human patients. In *C. elegans* this is done using transgenic animal with key UPR^{mt} proteins fused to

GFP while in mice it is done by performing western blots in lysed heart tissues of mice that have been following the experimental pipeline described in the *in vivo* validation section of this report.

It is known that UPR^{mt} functions by upregulating the transcription of key mitochondrial chaperones such as HSP-6 and HSP-60[97]. We can therefore use transgenic worms with fluorescently tagged HSP-6 or HSP-60 to allow for a quantitative readout of its expression. Commercially available strands are used to reduce costs and accelerate screening. The transgenic worms are then fed the different tetracycline derivatives to be screened and the fluorescence emitted by animals overexpressing HSP-6 and HSP-60 is measured and used to assess if a given drug induces UPR^{mt} activation. The process is automated using a microfluidic device to allow for a high-throughput screening[55].

In mice the expression of proteins known to be highly expressed in UPR^{mt} are assessed by western Blot. The analyzed proteins are HSPA9, a mitochondrial chaperone protein, LONP1, a mitochondrial protease, ASNS, an asparagine synthetase, as well as ELF2a and phosphorylated ELF2a (p-ELF2a) as it is known to favor ATF4 expression which in turns activates the UPR^{mt} pathway[55,98]. A detected overexpression of these proteins allows us to conclude that the chosen drug can activate the UPR^{mt} pathway *in vivo* in mice.

Together with the tests on AC16 cardiac cell lines during *in vitro* screening (section 3.4.6), this gives us high confidence in the ability of the drug to activate the pathway in human patients.

4.5 Pharmacokinetic (PK) and pharmacodynamic profiling in healthy dogs

Before a new drug can be tested on humans, preclinical testing to determine its safety and efficacy needs to be performed. After the selection of the most promising compounds in terms of efficiency and toxicity in mouse models, safety evaluation is performed on non-rodent species to increase the applicability of the test for human application[99]. Since the older diseased human heart may resemble that of a dog[29], dogs are widely used as a valuable non-rodent species for cardiovascular disease. Beagles are often selected, due to their cooperativity and availability, as well as for their small size and blood sampling[100], since they have a larger volume of blood than mice, so more blood can be taken.

Therefore, PK studies and toxicity assessments is performed on dogs for 24 weeks through daily oral administration. To evaluate the dose proportionality, multiples parameters are determined including the maximum concentration (C_{max}), the time of maximum concentration (T_{max}), the volume distribution (V_{ss}), the clearance (CL), the terminal elimination half time ($T_{1/2}$) and the bioavailability (F)[101]. Similarly, to what has been done in mice (sections 4.2 and 4.3.2), 3 groups of dogs are administered with low, medium, and high doses of compounds, with a fourth group being the control group. The left ventricular chamber and wall stiffness is measured by echocardiography, the mitochondrial bioenergetics are assessed by NMR spectroscopy and blood samples are collected weekly to measure biomarkers levels, such as natriuretic peptides, TIMP-1, and PAI-1. Moreover, as tetracyclines are a class of antibiotics that target bacterial translation, they also target mitochondrial translation and impair mitochondrial function[102]. Because mitochondrial metabolism plays a central role in the reallocation of nutrients for biomass production, tetracyclines are relevant for cancer research[103]. Therefore, the non-oncogenicity aspect, particularly for breast and prostate cancer[104], must be assessed on dogs before the human clinical trials start. At the end of this testing, the most promising molecule is selected to enter clinical trials.

5. Clinical trials

5.1 Phase I

The goal of phase I is to evaluate the drug's toxicity as well as its most frequent and serious adverse events. For this, we perform a dose escalation study on 25 to 35 healthy males and females between 18 and 60 years old. Pregnant women and people already under ongoing treatment are excluded, as the participants should be exposed to minimal risk.

We use four cohorts, in which volunteers are randomly assigned. The participants are blinded to the drug at each dose level and the total duration of this first phase is approximately 1 year.

The Starting Dose (SD) is determined from animal experiments mentioned in the previous section. The Human Equivalent Dose (HED) in [mg/kg] is determined from the No Observe Adverse Effect Level (NOAEL) found in animals, and from the body weight to body surface ratio in [kg/m^2], noted km. The HED is calculated as[105]: $HED = NOAEL * (km_{animal} / km_{human})$. For safety, the SD is set to the HED divided by a factor of 10 and sub-ministered to the first cohort. Then, the dose is gradually increased, according to the traditional 3+3 design[106] (Fig. 6 & Table 1). The highest dose administrated is kept as the Maximum Tolerated Dose (MTD).

Table 1. Dose levels of the first escalation study

Cohort 1	Cohort 2	Cohort 3	Cohort 4
SD	2*SD	3*SD	4*SD

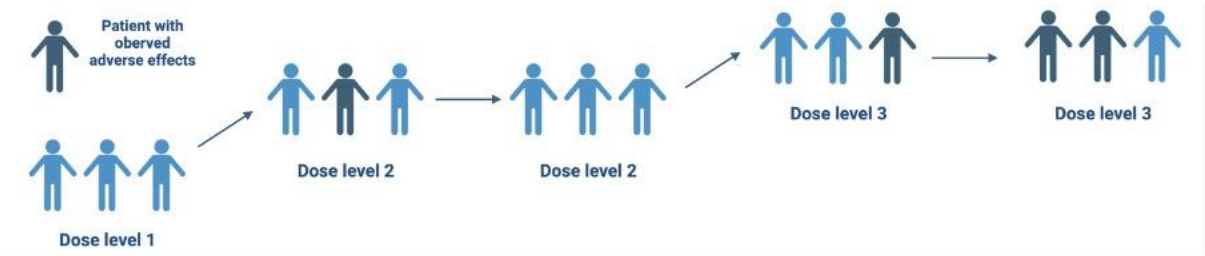

Figure 9. Design of the escalation study**.** Created with Biorender.com The 3+3 design is a traditionally used design in interventional clinical studies. 3 patients receive the dose. If no adverse effect is observed, 3 other patients receive the next dose; otherwise, the dose is tested on three other patients. If one of the participants experience adverse effect, the trial stops. If not, three other participants are administrated the next dose level and the study goes on[106].

Toxicity of the drug is determined thanks to several outcome measurements (Table 2) collected during several medical visits. First, a medical visit is held two days before the first dose administration to determine a baseline. Then, safety data are collected on day 0, 1 and 2 after each dose administration. Within 2 weeks after the treatment, every patient is also asked to fill a follow-up questionnaire on potential side-effects of tetracyclines administration such as abdominal discomfort, epigastric pain, nausea, vomiting[107].

Table 2. Primary outcome measurements performed during medical visits. These outcome measurements are also examined in medical visits during phase II and III.

Outcome measurement	Justification
Systolic and diastolic blood pressure, pulse rate, 12-lead electrocardiogram	To examine the safety and tolerability of the drug.
Physical examination	To assess any clinically significant abnormal physical examination findings after administration of the drug.

Hematology: differential and absolute hematocrit count, hemoglobin, mean corpuscular hemoglobin, mean corpuscular hemoglobin concentration, mean corpuscular volume, platelets, blood cells count.	To assess the hematology measurements as variables of safety and tolerability after administration of the drug.
Serum clinical chemistry: albumin, C-reactive protein, creatine kinase, creatinine, calcium, potassium, phosphate, sodium, urea and uric acid, liver enzymes, bilirubin, steroid.	To assess the serum clinical chemistry measurements as variables of safety and tolerability after administration of the drug.
HFpEF biomarkers blood levels: Plasminogen Activator Inhibitor (PAI-1), Tissue Inhibitor of Metalloproteinases (TIMP-1) and natriuretic acid peptide.	PAI-1 level is a good prognostic tool in HFpEF[108] . High blood levels of TIMP-1 are associated with fibrosis[109]. High blood levels of natriuretic peptide are associated with myocyte stress[109].

After this first escalation study, a second trial is held to control for the toxicity of the drug upon longer exposition. A 3+3 design[106] is used (Fig. 6 & Table 3). Three cohorts of 8 to 10 healthy males and females between 18 and 60 years old receive the treatment for 1 month, followed by 1 month of observation.

Table 3. Dose levels of the second escalation study.

Cohort 1	Cohort 2	Cohort 3
50% of MTD	75% of MTD	100% of MTD

The outcome measurements are the same as for the first escalation study (Table 2). The last given dosage is selected as the maximum dosage given in phase II and referred to as the Maximum Long-Term Tolerated Dosage (MLTTD).

5.2 Phase II

As the goal of phase II is to determine the drug effectiveness, a triple blinded (participants, care provider, investigator) randomized parallel assignment is conducted on 130 to 150 males and females with HFpEF. The selected participants are characterized by ≥ 40% ejection fraction and hypertension, and by an age 45 years old or older. Pregnant women and subjects under ongoing treatments are excluded. This phase is expected to last less than 3 years.

Participants are randomly divided in 4 cohorts. Each cohort comprises 5 subjects receiving placebo, while the other subjects are administered a fraction of the drug MLTTD once a day through an oral tablet and for a total duration of for 24 weeks (Table 4).

Table 4. Dosages of the phase II study. Each cohort comprises 32 to 38 participants.

Cohort 1	Cohort 2	Cohort 3	Cohort 4
25% of MTTLD	50% of MTTLD	75% of MTTLD	100% of MTTLD

HFpEF symptoms mainly affect the daily-basis functional capacity and life quality of the patients[110]. Thus, to test for the drug dosage efficacy on daily-life activities, patients are required to answer to the Kansas City Cardiomyopathy Questionnaire (KCCQ) and to perform a 6-minutes walking test (6MWT) within 1 week before the treatment and 1 week after the end of the treatment (Fig. 7). KCCQ is a 23-items questionnaire quantifying physical limitations, symptoms, self-efficacy, social interference, and quality of life[111]. Moreover, participants undergo a Cardiopulmonary Exercise Testing (CPET)[112] to measure their exercise ability, coupled to a Positron Emission Tomography (PET) scan[113]. CPET is commonly used to diagnose HFpEF as it allows to qualitatively and quantitively measure the origin of dyspnea, a common HFpEF symptom[112]. PET scan allows to test the presence of metabolic dysfunctions which are strongly associated with HFpEF and other frequently associated comorbidities (like diabetes, insulin resistance or aging), such as decreased glucose uptake[113]. Finally, echocardiography is also be performed one week before and one week after the treatment as it provides essential information on cardiac structure, function, and hemodynamics, which are critical features for HFpEF evaluation[114].

Safety and toxicity are assessed thanks to medical visits, where the same safety assessments as in phase I are performed (Table 2). One medical visit is held before the treatment, followed by medical visits every four weeks during treatment, and the last follow-up visit 4 weeks after the end of the treatment. Finally, subjects are tasked to fill out a follow-up questionnaire 8 weeks after the end of the treatment to report potential side effects (Fig. 7).

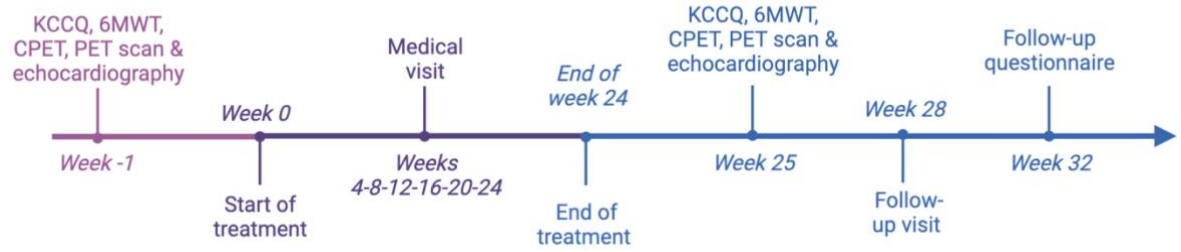

Figure 10. Phase II timeline. *Created with BioRender.com*

5.3 Phase III

In phase III of the clinical trials, the effect of the drug is evaluated on the exercise capacity in patients with HFpEF, as in phase II. Moreover, the aim is also to check for long-term or uncommon adverse effects. To do so, between 475 and 525 males and females with HFpEF with ≥ 40% ejection fraction and hypertension, 45 years old or older are involved in the study across several centers in Europe. Pregnant women and subjects under ongoing treatment are excluded. The study is expected to last 3 years.

Participants are randomly assigned to two cohorts, receiving either a placebo (1/10 of the participants) or the drug (9/10 of the participants) in an oral form daily for 24 weeks. The dosage of the drug is determined according to phase II of the clinical trial.

After 1 month of treatment, a medical visit is held to evaluate the patient's health and potential short-term toxic effects. To evaluate long-term adverse effects, participants undergo a control visit 3 months, 6 months, 1 year, and 2 years after the end of the treatment. During these medical visits, outcome measurements are evaluated as in phase I (Table 2).

The effects of the drug on the exercise capacity are assessed as in phase II thanks to KCCQ, 6MWT, CPET, PET scan, and echocardiography.

5.4 Phase IV

Phase IV consists of safety surveillance post-FDA approval. The goal is to gather more information on drug safety and effectiveness thanks to surveillance of spontaneously reported adverse effects. The phase IV is expected to last at least 3 years.

6. Business model

During the different steps of the drug discovery process, we designed each assay by considering multiple aspects, including the financial cost, and by selecting the cheapest assays if multiple analog ones were available. However, some costs could not be avoided such as the necessary machinery and the clinical trials procedures.

By considering all the experiments and machines, we reached an estimated total cost of 5.4 million US$ for the in vivo and in vitro assays for a duration between 4 and 5 years. The preclinical trial should last one year and cost 2 million US$, this includes the price of the animals, maintenance, the different tests, and experiments. The highest cost during the entire process is represented by the clinical trials, with the three phases of the trial expected to last approximately 6 years[115]. Previous drug development processes showed that the price for a cardiovascular trial is on average 39 857 US$ per patient[116]. In our trial we plan to enroll 30 patients in phase I, 240 patients in phase II, and 1000 patients in phase III, resulting in an estimated cost of our clinical trial of 51 million US$. Other expenses such as salaries have to be considered, rising the total cost between 74 and 183 million US$[116].

7. Conclusion

Activating the mitochondrial unfolded protein response in cardiomyocytes by targeting mitoribosomes is a promising key strategy to achieve cardioprotection and prevent HFpEF in hypertensive patients following myocardial infarction. The drug development process described in this report thus focuses on the identification of novel tetracycline drugs that impair mitoribosome function by inducing the UPR^{mt} in cardiomyocytes.

We first describe the virtual screening phase whose goal is to identify potential hit candidates, followed by *in vitro* primary assays to reduce the number of selected compounds based on diverse criteria such as solubility, intestinal permeability, toxicity, and ability to induce UPR^{mt}. Secondary toxicity assays, as well as optimization of the structure, are then depicted with the goal of further selecting the candidates that best match the defined criteria. We then justify our choice of mouse models for the *in vivo* validation tests and detail the experimental design in mice and healthy dogs to assess the efficacy of the drug candidates *in vivo*. The report finally describes the workflow of the clinical trials that aim at testing the safety and efficacy of our hit-to-lead choice in humans.

The strategy presented here allows us to eventually extend our studies to all hypertensive patients to prevent HFpEF, even without a previous episode of myocardial infarction. Because hypertension triggers a systemic pro-inflammatory state that can lead to heart dysfunction[15], the restoration of mitochondrion via the enhancement of the UPR^{mt} plays a protective role in the stressed heart[19]. Other comorbidities linked with HFpEF, such as diabetes mellitus or obesity that have similar features and biological mechanisms increasing the risk for HFpEF could also be future targets. Moreover, evidence showing the link between mitochondria and cardiovascular diseases is accumulating[18], suggesting that we could apply our strategy in preventing other heart diseases. For example, mitochondrial dysfunction is responsible for the initiation and progression of coronary artery disease (CAD), the leading cause of death in the developed world, mainly caused by excessive ROS production[117]. Therefore, investing in our research and development department can contribute to the establishment of tetracycline compounds targeting not only CAD but a multitude of cardiovascular diseases.

Bibliography

1. Savarese, G. *et al.* Global burden of heart failure: a comprehensive and updated review of epidemiology. *Cardiovasc Res* cvac013 (2022) doi:10.1093/cvr/cvac013.
2. Borlaug, B. A. & Paulus, W. J. Heart failure with preserved ejection fraction: pathophysiology, diagnosis, and treatment. *Eur Heart J* **32**, 670–679 (2011).
3. del Campo, A., Perez, G., Castro, P. F., Parra, V. & Verdejo, H. E. Mitochondrial function, dynamics and quality control in the pathophysiology of HFpEF. *Biochimica et Biophysica Acta (BBA) - Molecular Basis of Disease* **1867**, 166208 (2021).
4. Bozkurt, B. *et al.* Universal definition and classification of heart failure: a report of the Heart Failure Society of America, Heart Failure Association of the European Society of Cardiology, Japanese Heart Failure Society and Writing Committee of the Universal Definition o. *Eur J Heart Fail* **23**, 352–380 (2021).
5. Jenča, D. *et al.* Heart failure after myocardial infarction: incidence and predictors. *ESC Heart Fail* **8**, 222–237 (2021).
6. Kamon, D. *et al.* Predominant subtype of heart failure after acute myocardial infarction is heart failure with non-reduced ejection fraction. *ESC Heart Fail* **8**, 317–325 (2021).
7. Borlaug, B. A. The pathophysiology of heart failure with preserved ejection fraction. *Nat Rev Cardiol* **11**, 507–515 (2014).
8. Paulus, W. J. *et al.* How to diagnose diastolic heart failure: a consensus statement on the diagnosis of heart failure with normal left ventricular ejection fraction by the Heart Failure and Echocardiography Associations of the European Society of Cardiology. *Eur Heart J* **28**, 2539–2550 (2007).
9. Huis in 't Veld, A. E., de Man, F. S., van Rossum, A. C. & Handoko, M. L. How to diagnose heart failure with preserved ejection fraction: the value of invasive stress testing. *Netherlands Heart Journal* **24**, 244–251 (2016).
10. LeWinter, M. M. & Meyer, M. Mechanisms of Diastolic Dysfunction in Heart Failure With a Preserved Ejection Fraction. *Circ Heart Fail* **6**, 1112–1115 (2013).
11. Heinzel, F. R. & Shah, S. J. The future of heart failure with preserved ejection fraction. *Herz* **47**, 308–323 (2022).
12. Borlaug, B. A. Evaluation and management of heart failure with preserved ejection fraction. *Nat Rev Cardiol* **17**, 559–573 (2020).
13. Franssen, C., Chen, S., Hamdani, N. & Paulus, W. J. From comorbidities to heart failure with preserved ejection fraction: a story of oxidative stress. *Heart* **102**, 320 (2016).
14. Hicklin, H. E., Gilbert, O. N., Ye, F., Brooks, J. E. & Upadhya, B. Hypertension as a Road to Treatment of Heart Failure with Preserved Ejection Fraction. *Curr Hypertens Rep* **22**, 82 (2020).
15. Schiattarella, G. G. *et al.* Nitrosative stress drives heart failure with preserved ejection fraction. *Nature* **568**, 351–356 (2019).
16. Lopaschuk, G. D., Karwi, Q. G., Tian, R., Wende, A. R. & Abel, E. D. Cardiac Energy Metabolism in Heart Failure. *Circ Res* **128**, 1487–1513 (2021).
17. Knowlton, A. A., Chen, L. & Malik, Z. A. Heart Failure and Mitochondrial Dysfunction: The Role of Mitochondrial Fission/Fusion Abnormalities and New Therapeutic Strategies. *J Cardiovasc Pharmacol* **63**, (2014).
18. Poznyak, A. v, Ivanova, E. A., Sobenin, I. A., Yet, S.-F. & Orekhov, A. N. The Role of Mitochondria in Cardiovascular Diseases. *Biology* vol. 9 Preprint at https://doi.org/10.3390/biology9060137 (2020).
19. Smyrnias, I. *et al.* Cardioprotective Effect of the Mitochondrial Unfolded Protein Response During Chronic Pressure Overload. *J Am Coll Cardiol* **73**, 1795–1806 (2019).
20. Liu, J., He, X., Zheng, S., Zhu, A. & Wang, J. The Mitochondrial Unfolded Protein Response: A Novel Protective Pathway Targeting Cardiomyocytes. *Oxid Med Cell Longev* **2022**, 6430342 (2022).
21. Kenny, T. C., Manfredi, G. & Germain, D. The Mitochondrial Unfolded Protein Response as a Non-Oncogene Addiction to Support Adaptation to Stress during Transformation in

Cancer and Beyond . *Frontiers in Oncology* vol. 7 Preprint at https://www.frontiersin.org/articles/10.3389/fonc.2017.00159 (2017).
22. Houtkooper, R. H. *et al.* Mitonuclear protein imbalance as a conserved longevity mechanism. *Nature* **497**, 451 (2013).
23. Yun, J. & Finkel, T. Mitohormesis. *Cell Metab* **19**, 757–766 (2014).
24. Griffin, M. O., Ceballos, G. & Villarreal, F. J. Tetracycline compounds with non-antimicrobial organ protective properties: possible mechanisms of action. *Pharmacol Res* **63**, 102–107 (2011).
25. Greber, B. J. & Ban, N. Structure and Function of the Mitochondrial Ribosome. *Annu Rev Biochem* **85**, 103–132 (2016).
26. Chatzispyrou, I. A., Held, N. M., Mouchiroud, L., Auwerx, J. & Houtkooper, R. H. Tetracycline antibiotics impair mitochondrial function and its experimental use confounds research. *Cancer Res* **75**, 4446–4449 (2015).
27. Suárez-Rivero, J. M. *et al.* UPRmt activation improves pathological alterations in cellular models of mitochondrial diseases. *Orphanet J Rare Dis* **17**, 204 (2022).
28. Moullan, N. *et al.* Tetracyclines Disturb Mitochondrial Function across Eukaryotic Models: A Call for Caution in Biomedical Research. *Cell Rep* **10**, 1681–1691 (2015).
29. Hearse, D. J. & Sutherland, F. J. Experimental Models for the Study of Cardiovascular Function and Disease Defining the Question and Identifying the Model. *Pharmacol Res* **41**, (2000).
30. Butler, J. *et al.* Rationale and Design of the VITALITY-HFpEF Trial. *Circ Heart Fail* **12**, e005998 (2019).
31. Douguet, D. e-LEA3D: a computational-aided drug design web server. *Nucleic Acids Res* **38**, W615–W621 (2010).
32. Kim, S. *et al.* PubChem in 2021: new data content and improved web interfaces. *Nucleic Acids Res* **49**, D1388–D1395 (2021).
33. Korb, O., Stützle, T. & Exner, T. E. Empirical Scoring Functions for Advanced Protein−Ligand Docking with PLANTS. *J Chem Inf Model* **49**, 84–96 (2009).
34. Sapundzhi, F., Prodanova, K. & Lazarova, M. Survey of the scoring functions for protein-ligand docking. in 100008 (2019). doi:10.1063/1.5133601.
35. Amunts, A., Brown, A., Toots, J., Scheres, S. H. W. & Ramakrishnan, V. The structure of the human mitochondrial ribosome. *Science (1979)* **348**, 95–98 (2015).
36. Kaushal, P. S. *et al.* Cryo-EM structure of the small subunit of the mammalian mitochondrial ribosome. *Proceedings of the National Academy of Sciences* **111**, 7284–7289 (2014).
37. Chukwudi, C. U. rRNA Binding Sites and the Molecular Mechanism of Action of the Tetracyclines. *Antimicrob Agents Chemother* **60**, 4433–4441 (2016).
38. Schrödinger, L. & DeLano, W. PyMOL. Retrieved from http://www.pymol.org/pymol. Preprint at (2020).
39. DOCK. Preprint at https://dock.compbio.ucsf.edu.
40. MolSoft. ICM.
41. SimulationsPlus. ADMET Predictor®. Preprint at https://www.simulations-plus.com/software/admetpredictor/.
42. Rube, H. T. *et al.* Prediction of protein–ligand binding affinity from sequencing data with interpretable machine learning. *Nat Biotechnol* **40**, 1520–1527 (2022).
43. Ertl, P. & Schuffenhauer, A. Estimation of synthetic accessibility score of drug-like molecules based on molecular complexity and fragment contributions. *J Cheminform* **1**, 8 (2009).
44. Creative Biolabs. Solubility Assay. https://www.creative-biolabs.com/solubility-assay.html.
45. Kerns, E., Di, L. & Carter, G. In Vitro Solubility Assays in Drug Discovery. *Curr Drug Metab* **9**, 879–885 (2008).
46. Creative Biolabs. Expedite Your PROTAC® Research everywhere, every day. https://www.creative-biolabs.com/protac/cell-permeability-

efficacy.htm?gclid=EAIaIQobChMIz_mg05ic-wIVC95RCh0cdwpTEAAYAiAAEgJwwPD_BwE.
47. Cyprotex. Caco-2 Permeability Assay. https://www.cyprotex.com/admepk/in-vitro-permeability-and-drug-transporters/caco-2-permeability.
48. van Breemen, R. B. & Li, Y. Caco-2 cell permeability assays to measure drug absorption. *Expert Opin Drug Metab Toxicol* **1**, 175–185 (2005).
49. Brian, H., Victoria E., C. F., Joseph R., L., Thomas J., F. & Michael W., D. Fluorescence Resonance Energy Transfer (FRET) Microscopy. https://www.olympus-lifescience.com/en/microscope-resource/primer/techniques/fluorescence/fret/fretintro/.
50. An, W. F. Fluorescence-Based Assays. in *Cell-Based Assays for High-Throughput Screening: Methods and Protocols* (eds. Clemons, P. A., Tolliday, N. J. & Wagner, B. K.) 97–107 (Humana Press, 2009). doi:10.1007/978-1-60327-545-3_7.
51. Leavesley, S. J. & Rich, T. C. Overcoming limitations of FRET measurements. *Cytometry Part A* **89**, 325–327 (2016).
52. Prashansa, A. NMR Spectroscopy in Drug Discovery and Development. *MATER METHODS* **4**, 599 (2014).
53. Vanwetswinkel, S. *et al.* TINS, Target Immobilized NMR Screening: An Efficient and Sensitive Method for Ligand Discovery. *Chem Biol* **12**, 207–216 (2005).
54. Davidson, M. M. *et al.* Novel cell lines derived from adult human ventricular cardiomyocytes. *J Mol Cell Cardiol* **39**, 133–147 (2005).
55. Mottis, A. *et al.* Tetracycline-induced mitohormesis mediates disease tolerance against influenza. *J Clin Invest* **132**, (2022).
56. Forloni, M., Liu, A. Y. & Wajapeyee, N. Methods for in vitro Mutagenesis. *Cold Spring Harb. Protoc.* **2019**, db.top097733 (2019).
57. Eastmond, D. A. *et al.* Mutagenicity testing for chemical risk assessment: update of the WHO/IPCS Harmonized Scheme. *Mutagenesis* **24**, 341–349 (2009).
58. Mortelmans, K. & Zeiger, E. The Ames Salmonella/microsome mutagenicity assay. *Mutation Research/Fundamental and Molecular Mechanisms of Mutagenesis* **455**, 29–60 (2000).
59. Nijman, S. M. B. Synthetic lethality: general principles, utility and detection using genetic screens in human cells. *FEBS Lett.* **585**, 1–6 (2011).
60. Nijman, S. M. B. Synthetic lethality: general principles, utility and detection using genetic screens in human cells. *FEBS Lett.* **585**, 1–6 (2011).
61. Festag, M., Viertel, B., Steinberg, P. & Sehner, C. An in vitro embryotoxicity assay based on the disturbance of the differentiation of murine embryonic stem cells into endothelial cells. II. Testing of compounds. *Toxicology in Vitro* **21**, 1631–1640 (2007).
62. Seiler, A. E. M. & Spielmann, H. The validated embryonic stem cell test to predict embryotoxicity in vitro. *Nat Protoc* **6**, 961–978 (2011).
63. Estevan, C., C., A., Pamies, D., Vilanova, E. & A., M. Embryonic Stem Cells in Toxicological Studies. in *Embryonic Stem Cells - Basic Biology to Bioengineering* (InTech, 2011). doi:10.5772/24804.
64. REACTION BIOLOGY. Target-specific Assays: Kinase Assays. https://www.reactionbiology.com/services/kinase-assays/kinase-screening?gclid=Cj0KCQiA4aacBhCUARIsAI55maGb3JIhlleDEEV3Wrw6_yN3Js4Kk4g9v1Vi2zrG3bPTODjNvRDf18YaArXREALw_wcB.
65. Ishigami-Yuasa, M. & Kagechika, H. Chemical Screening of Nuclear Receptor Modulators. *Int J Mol Sci* **21**, 5512 (2020).
66. Bayot, M. & Bragg, B. Antimicrobial Susceptibility Testing. *Treasure Island (FL): StatPearls Publishing* https://www.ncbi.nlm.nih.gov/books/NBK539714/?report=classic (2022).
67. Bárcena, C., Mayoral, P. & Quirós, P. M. Mitohormesis, an Antiaging Paradigm. in 35–77 (2018). doi:10.1016/bs.ircmb.2018.05.002.
68. Liu, H. *et al.* Comparing the disk-diffusion and agar dilution tests for Neisseria gonorrhoeae antimicrobial susceptibility testing. *Antimicrob Resist Infect Control* **5**, 46 (2016).

69. Sagar, A. McFarland Standards- Principle, Preparation, Uses, Limitations. *Microbe Notes* https://microbenotes.com/mcfarland-standards/ (2021).
70. Markossian, S., Grossman, A., Brimacombe, K. & et al. *Assay Guidance Manual*. vol. Bethesda (MD) (2004).
71. UNIL. Volume of distribution. *PHARMACOKINETICS: Online content for student* https://sepia2.unil.ch/pharmacology/parameters/volumeofdistribution/.
72. Zhang, D., Luo, G., Ding, X. & Lu, C. Preclinical experimental models of drug metabolism and disposition in drug discovery and development. *Acta Pharm Sin B* **2**, 549–561 (2012).
73. SATOSHI, I. Why You Need QWBA for Human Radiolabeled ADME Studies. *XenoTech: Drug Development Insights* https://www.xenotech.com/blog/why-you-need-qwba-for-human-radiolabeled-adme-studies/.
74. Azure Biosystems. PHOSPHOR IMAGING. https://azurebiosystems.com/western-blotting-applications/phosphor-imaging/.
75. Suárez-Rivero, J. M. *et al.* Activation of the Mitochondrial Unfolded Protein Response: A New Therapeutic Target? *Biomedicines* **10**, 1611 (2022).
76. Jain, A. K. & Pandey, A. K. In Vivo Micronucleus Assay in Mouse Bone Marrow. in *Genotoxicity Assessment: Methods and Protocols* (eds. Dhawan, A. & Bajpayee, M.) 135–146 (Springer New York, 2019). doi:10.1007/978-1-4939-9646-9_7.
77. *Test No. 474: Mammalian Erythrocyte Micronucleus Test*. (OECD, 2016). doi:10.1787/9789264264762-en.
78. INTERNATIONAL CONFERENCE ON HARMONISATION OF TECHNICAL REQUIREMENTS FOR REGISTRATION OF PHARMACEUTICALS FOR HUMAN USE. GUIDANCE ON GENOTOXICITY TESTING AND DATA INTERPRETATION FOR PHARMACEUTICALS INTENDED FOR HUMAN USE S2(R1). *ICH HARMONISED TRIPARTITE GUIDELINE* https://database.ich.org/sites/default/files/S2%28R1%29%20Guideline.pdf (2011).
79. INTERNATIONAL CONFERENCE ON HARMONISATION OF TECHNICAL REQUIREMENTS FOR REGISTRATION OF PHARMACEUTICALS FOR HUMAN USE. IMMUNOTOXICITY STUDIES FOR HUMAN PHARMACEUTICALS S8. *ICH HARMONISED TRIPARTITE GUIDELINE* https://database.ich.org/sites/default/files/S8_Guideline_0.pdf (2005).
80. INTERNATIONAL CONFERENCE ON HARMONISATION OF TECHNICAL REQUIREMENTS FOR REGISTRATION OF PHARMACEUTICALS FOR HUMAN USE. NOTE FOR GUIDANCE ON TOXICOKINETICS: THE ASSESSMENT OF SYSTEMIC EXPOSURE IN TOXICITY STUDIES S3A. *ICH HARMONISED TRIPARTITE GUIDELINE* https://database.ich.org/sites/default/files/S3A_Guideline.pdf (1994).
81. INTERNATIONAL COUNCIL FOR HARMONISATION OF TECHNICAL REQUIREMENTS FOR PHARMACEUTICALS FOR HUMAN USE. DETECTION OF REPRODUCTIVE AND DEVELOPMENTAL TOXICITY FOR HUMAN PHARMACEUTICALS S5(R3). *ICH HARMONISED GUIDELINE* https://database.ich.org/sites/default/files/S5-R3_Step4_Guideline_2020_0218_1.pdf (2020).
82. Tu, P. *et al.* Gut Microbiome Toxicity: Connecting the Environment and Gut Microbiome-Associated Diseases. *Toxics* **8**, 19 (2020).
83. Valero-Muñoz, M., Backman, W. & Sam, F. Murine Models of Heart Failure With Preserved Ejection Fraction: A “Fishing Expedition”. *JACC Basic Transl Sci* **2**, 770–789 (2017).
84. Valero-Muñoz, M. *et al.* Heart Failure With Preserved Ejection Fraction Induces Beiging in Adipose Tissue. *Circ Heart Fail* **9**, e002724 (2016).
85. Wilson, R. M., de Silva, D. S., Sato, K., Izumiya, Y. & Sam, F. Effects of fixed-dose isosorbide dinitrate/hydralazine on diastolic function and exercise capacity in hypertension-induced diastolic heart failure. *Hypertension* **54**, 583–590 (2009).

86. Qin, W. *et al.* Transgenic Model of Aldosterone-Driven Cardiac Hypertrophy and Heart Failure. *Circ Res* **93**, 69–76 (2003).
87. Valero-Muñoz, M., Backman, W. & Sam, F. Murine Models of Heart Failure With Preserved Ejection Fraction: A “Fishing Expedition”. *JACC Basic Transl Sci* **2**, 770–789 (2017).
88. Peng, H. *et al.* Angiotensin II-induced dilated cardiomyopathy in Balb/c but not C57BL/6J mice. *Exp Physiol* **96**, 756–764 (2011).
89. Sawall, S. *et al. In Vivo* Quantification of Myocardial Infarction in Mice Using Micro-CT and a Novel Blood Pool Agent. *Contrast Media Mol Imaging* **2017**, 2617047 (2017).
90. Sam, F. *et al.* Progressive left ventricular remodeling and apoptosis late after myocardial infarction in mouse heart. *American Journal of Physiology-Heart and Circulatory Physiology* **279**, H422–H428 (2000).
91. Petrosino, J. M. *et al.* Graded Maximal Exercise Testing to Assess Mouse Cardio-Metabolic Phenotypes. *PLoS One* **11**, e0148010- (2016).
92. Villalba-Orero, M., Garcia-Pavia, P. & Lara-Pezzi, E. Non-invasive assessment of HFpEF in mouse models: current gaps and future directions. *BMC Med* **20**, 349 (2022).
93. Carnes, J. & Gordon, G. Biomarkers in Heart Failure With Preserved Ejection Fraction: An Update on Progress and Future Challenges. *Heart Lung Circ* **29**, 62–68 (2020).
94. Withaar, C., Lam, C. S. P., Schiattarella, G. G., de Boer, R. A. & Meems, L. M. G. Heart failure with preserved ejection fraction in humans and mice: embracing clinical complexity in mouse models. *Eur Heart J* **42**, 4420–4430 (2021).
95. González, A. *et al.* Filling Pressures and Collagen Metabolism in Hypertensive Patients With Heart Failure and Normal Ejection Fraction. *Hypertension* **55**, 1418–1424 (2010).
96. Vaughan, D. E., Rai, R., Khan, S. S., Eren, M. & Ghosh, A. K. Plasminogen Activator Inhibitor-1 Is a Marker and a Mediator of Senescence. *Arterioscler Thromb Vasc Biol* **37**, 1446–1452 (2017).
97. Yoneda, T. *et al.* Compartment-specific perturbation of protein handling activates genes encoding mitochondrial chaperones. *J Cell Sci* **117**, 4055–4066 (2004).
98. D’Amico, D., Sorrentino, V. & Auwerx, J. Cytosolic Proteostasis Networks of the Mitochondrial Stress Response. *Trends Biochem Sci* **42**, 712–725 (2017).
99. Son, Y.-W., Choi, H.-N., Che, J.-H., Kang, B.-C. & Yun, J.-W. Advances in selecting appropriate non-rodent species for regulatory toxicology research: Policy, ethical, and experimental considerations. *Regulatory Toxicology and Pharmacology* **116**, 104757 (2020).
100. Son, Y.-W., Choi, H.-N., Che, J.-H., Kang, B.-C. & Yun, J.-W. Advances in selecting appropriate non-rodent species for regulatory toxicology research: Policy, ethical, and experimental considerations. *Regulatory Toxicology and Pharmacology* **116**, 104757 (2020).
101. Zhang, D., Luo, G., Ding, X. & Lu, C. Preclinical experimental models of drug metabolism and disposition in drug discovery and development. *Acta Pharm Sin B* **2**, 549–561 (2012).
102. Chatzispyrou, I. A., Held, N. M., Mouchiroud, L., Auwerx, J. & Houtkooper, R. H. Tetracycline Antibiotics Impair Mitochondrial Function and Its Experimental Use Confounds Research. *Cancer Res* **75**, 4446–4449 (2015).
103. Wallace, D. C. Mitochondria and cancer. *Nat Rev Cancer* **12**, 685–698 (2012).
104. Duivenvoorden, W. C., Hirte, H. W. & Singh, G. Use of tetracycline as an inhibitor of matrix metalloproteinase activity secreted by human bone-metastasizing cancer cells. *Invasion & metastasis* **17**, 312–322 (1997).
105. U.S. Department of Health and Human Services Food and Drug Administration Center for Drug Evaluation and Research (CDER). Guidance for Industry Estimating the Maximum Safe Starting Dose in Initial Clinical Trials for Therapeutics in Adult Healthy Volunteers. https://www.fda.gov/media/72309/download (2005).
106. Shen, J. *et al.* Design and Conduct Considerations for First-in-Human Trials. *Clin Transl Sci* **12**, 6 (2019).

107. Shutter, M. C. & Akhondi, H. Tetracycline. *Kucers the Use of Antibiotics: A Clinical Review of Antibacterial, Antifungal, Antiparasitic, and Antiviral Drugs, Seventh Edition* 1195–1203 (2022) doi:10.1201/9781315152110.
108. Winter, M. P. *et al.* Prognostic significance of tPA/PAI-1 complex in patients with heart failure and preserved ejection fraction. *Thromb Haemost* **117**, 471–478 (2017).
109. Meijers, W. C., van der Velde, A. R. & de Boer, R. A. Biomarkers in heart failure with preserved ejection fraction. *Netherlands Heart Journal* **24**, 252 (2016).
110. Butler, J. *et al.* Exploring New Endpoints for Patients with Heart Failure with Preserved Ejection Fraction. *Circ Heart Fail* **9**, (2016).
111. Green, C. P., Porter, C. B., Bresnahan, D. R. & Spertus, J. A. Development and evaluation of the Kansas City Cardiomyopathy Questionnaire: a new health status measure for heart failure. *J Am Coll Cardiol* **35**, 1245–1255 (2000).
112. Guazzi, M. *et al.* Exercise testing in heart failure with preserved ejection fraction: an appraisal through diagnosis, pathophysiology and therapy – A clinical consensus statement of the Heart Failure Association and European Association of Preventive Cardiology of the European Society of Cardiology. *Eur J Heart Fail* **24**, 1327–1345 (2022).
113. Li, Z., Gupte, A. A., Zhang, A. & Hamilton, D. J. Pet Imaging and its Application in Cardiovascular Diseases. *Methodist Debakey Cardiovasc J* **13**, 29 (2017).
114. Obokata, M., Reddy, Y. N. V. & Borlaug, B. A. The Role of Echocardiography in Heart Failure with Preserved Ejection Fraction. *Heart Fail Clin* **15**, 241–256 (2019).
115. Sofpromed. How Much Does a Clinical Trial Cost? https://www.sofpromed.com/how-much-does-a-clinical-trial-cost#:~:text=The%20cost%20of%20a%20clinical,per%20protocol%2C%20among%20other%20aspects.).
116. Moore, T. J., Heyward, J., Anderson, G. & Alexander, G. C. Variation in the estimated costs of pivotal clinical benefit trials supporting the US approval of new therapeutic agents, 2015–2017: a cross-sectional study. *BMJ Open* **10**, e038863 (2020).
117. Siasos, G. *et al.* Mitochondria and cardiovascular diseases—from pathophysiology to treatment. *Ann Transl Med* **6(12)**, 256 (2018).

Supplementary material

Supplementary Table 1. LEA3D parameters used for virtual screening and *de novo* small molecule design.

Parameter name	Minimal value	Maximal value	Weight in final score	Comment
binding site radius	35		0.8	rather big (arbitrary)
reference mol	tetracycline.sdf		0.8	from PubChem (https://pubchem.ncbi.nlm.nih.gov/compound/Tetracycline)
Molecular weight	400	650	0.8	Tetracycline molecular weight=444, leave flexibility for new fragments
Number of atoms (H excluded)	20	40	0.4	Tetracycline Number of atoms=38 (noH)
Number of H-donors	0	4	0.8	Relatively flexible
Number of H-acceptors	0	8	0.8	Relatively flexible
Polar solvent accessible surface area	0	140	0.4	Veber's rule
Fraction of sp3-hybridized C	-	-	0	-
Volume	-	-	0	-
Area	-	-	0	-
Number of rotatable bonds	0	8	0.4	Veber's rule
Number of rings	0	2	0.4	Tetracycline has 4 aromatic rings, leave a little bit of flexibilty for new rings
Number of aromatic rings	4	6	0	Tetracycline has 4 aromatic rings, leave a little bit of flexibilty for new rings